Quantifying the role of moss in terrestrial ecosystem carbon dynamics in northern high-latitudes

Junrong Zha and Qianlai Zhuang

Department of Earth, Atmospheric, and Planetary Sciences and Department of Agronomy,
Purdue University, West Lafayette, IN 47907, USA

Correspondence: Qianlai Zhuang (qzhuang@purdue.edu)

To be submitted to: *Journal of Biogeoscience*

Key words: moss, carbon dynamics, Earth System Modeling, terrestrial ecosystems, Arctic

Abstract

Mosses are ubiquitous in northern terrestrial ecosystems, and play an important role in regional carbon, water and energy cycling. Current global land surface models that do not consider mosses may bias the quantification of regional carbon dynamics. Here we incorporate mosses as a new plant functional type into the process-based Terrestrial Ecosystem Model (TEM 5.0), to develop a new model (TEM_Moss). The new model explicitly quantifies the interactions between vascular plants and mosses and their competition for energy, water, and nutrients. Compared to the estimates using TEM 5.0, the new model estimates that the regional terrestrial soils currently store 132.7 Pg more C, and will store 157.5 Pg and 179.1 Pg more C under the RCP 8.5 and RCP 2.6 scenarios, respectively, by the end of the 21st century. Ensemble regional simulations forced with different parameters for the 21st century with TEM_Moss predict that the region will accumulate 161.1±142.1 Pg C under the RCP 2.6 scenario, and 186.7±166.1 Pg C under the RCP 8.5 scenario over the century. Our study highlights the necessity of coupling moss into Earth System Models to adequately quantify terrestrial carbon-climate feedbacks in the Arctic.

1. Introduction

Northern high latitude ecosystems, which refers to the land ecosystems (>45 ºN) in northern temperate, boreal, grassland and tundra regions, hold about 30% of global terrestrial carbon (C) in soils and plants (Allison and Treseder, 2008; Jobbágy and Jackson, 2000; Kasischke, 2000; Tarnocai et al., 2009; Hugelius et al., 2014), and contain as much as 1024 Pg soil organic carbon from 0 to 3 m depth (Treseder et al., 2016; Schuur et al., 2008). This large amount of carbon is potentially responsive to ongoing global warming (Burke et al., 2017, Koven et al., 2015, Comyn-Platt et al., 2018)), which is especially pronounced at high latitudes (Treseder et al., 2016; IPCC, 2014). Thus, explicit investigation of carbon-climate feedback is important (Wieder et al., 2013; Bond-Lamberty and Thomson, 2010).

Ecosystem models are important tools for understanding the role of boreal ecosystems in carbon-climate feedbacks (Bond-Lamberty et al., 2005; Chadburn et al., 2017; Zhuang et al., 2002; Treseder et al., 2016). Process-based biogeochemical models such as TEM (Hayes et al., 2014; Raich et al., 1991; Melillo et al., 1993; McGuire et al., 1992; Zhuang et al., 2001, 2002, 2010, 2013), Biome-BGC (Running and Coughlan, 1988; Bond-Lamberty et al., 2007), and Biosphere Energy Transfer Hydrology scheme (BETHY) (Knorr, 2000) are increasingly employed to simulate current and future carbon dynamics. Those models estimate carbon dynamics by simulating processes such as photosynthesis, respiration, nitrogen competition, evapotranspiration and soil decomposition (Bond-Lamberty et al., 2005; Zhuang et al., 2015). The results from these models are influenced by components and processes that are built into the model (Turetsky et al., 2012; Oreskes et al., 1994). However, the role of boreal forests in carbon sink or source activities has not yet reached a consensus due to a number of model limitations (Cahoon et al., 2012; Hayes et al., 2011; Todd-Brown et al., 2013).

63   One limitation is that ecosystems models often ignore some important components such

64   as understory processes that play crucial roles in biogeochemical cycles (Zhuang et al., 2002;

65   Treseder et al., 2011; Bond-Lamberty et al., 2005). For instance, mosses are ubiquitous in

66   northern ecosystems, and show a pattern of increasing abundance with increasing latitude

67   (Turetsky et al., 2012; Jägerbrand et al., 2006). Their functional traits, including tolerance to

68   drought and a broad response of net assimilation rates to temperature, allow them to persist in

69   high-latitude regions (Kallio and Heinonen, 1975; Harley et al., 1989). The activities of moss

70   that are related to water, nutrients, and energy may influence several ecosystem processes such

71   as permafrost formation and thaw, peat accumulation, soil decomposition and net primary

72   productivity (NPP) (Turetsky et al., 2012; Nilsson and Wardle, 2005). Mosses can have positive

73   or negative interactions with vascular plants (Skre and Oechel, 1979; Turetsky et al., 2010). On

74   the one hand, mosses compete with vascular plants for available nutrients, negatively affecting

75   vascular plants productivity (Skre and Oechel, 1979; Gornall et al., 2011; Turetsky et al., 2012).

76   Besides, a thick moss cover can form an environment with water logging or low oxygen supply,

77   which is common in high-latitude regions (Skre and Oechel, 1979; Cornelissen et al., 2007). The

78   moss cover prevents absorbed solar heat from being conducted down into the soil, and tends to

79   decrease soil temperature in summer. Therefore, soil decomposition rates can be affected since

80   they are mediated by soil temperature, which will further influence growth of vascular plants

81   (Gornall et al., 2007). On the other hand, some species of mosses can serve as an important

82   source of nitrogen because of their associations with microbial nitrogen fixers (Basilier, 1979;

83   DeLuca et al., 2007; Markham, 2009; Kip et al., 2011). Thus, mosses can also exert positive

84   effects on plant growth due to their regulation of nitrogen availability for vascular plants (Hobbie

85   et al., 2000; Gornall et al., 2007). It is gradually being recognized that mosses can have

86   comparable influences on high-latitude ecosystems to vascular plants, due to their large density

87   and essential function in plant competition, soil climate, and carbon and nutrient cycling

88   (Longton, 1988; Lindo and Gonzalez, 2010; Okland, 1995; Pharo and Zartman, 2007). They can

89   on average contribute 20% of aboveground NPP in boreal forests (Turetsky et al., 2010), and

90   their annual NPP may reach as high as 350 g C m^{-2} in some regions in the Arctic (Pakarinen and

91   Vitt 1973), even exceeding that of vascular plants (Oechel and Collins, 1976; Clarke et al.,

92   1971). Thus, ignorance of mosses, the keystone species of boreal ecosystems, can pose large

93   biases in model predictions and limit the utility of models. To date, a number of ecosystem

94   models have already included moss activities to explore the response of moss to disturbance

95   (Bond-Lamberty et al., 2007; Euskirchen et al., 2009; Frolking et al., 2010, Wania et al., 2009,

96   Chadburn et al., 2015, Porada et al., 2016, Druel et al., 2017), or improve model prediction of

97   carbon dynamics (Bond-Lamberty et al., 2005). However, the potential role of moss in the

98   regional carbon dynamics in northern high latitudes has been slowly evaluated by considering

99   the interactions between moss and vascular plants, especially with respect to their competition

100   for water, nutrient and energy.

101   This study developed a new version of Terrestrial Ecosystem Model (Raich et al., 1991;

102   McGuire et al., 1992; Zhuang et al., 2001, 2002, 2010, 2013, 2015), hereafter referred to as

103   TEM_Moss, by explicitly considering moss impacts on terrestrial ecosystem carbon dynamics.

104   The competition of water, energy and nutrient between vascular plants and mosses are explicitly

105   modeled. The verified TEM_Moss and previous TEM were compared against the observed data of

106   ecosystem carbon, soil temperature and moisture dynamics. Both models were then used to analyze

107   the regional carbon dynamics in northern high latitudes (north of 45 °N) during the 20th and 21st

108   centuries.

2. Methods

2.1 Overview

First, we briefly describe how we developed the TEM_Moss by modifying the previous TEM 5.0 to consider their interactions between vascular plants and mosses. Second, parameterization and validation of TEM_Moss using measured gap-filled carbon flux data and meteorological data at representative sites is presented. Third, we present how we have applied both models (TEM_Moss and TEM 5.0) to the northern high latitudes (above 45 °N) to quantify regional carbon dynamics during the 20th and 21st centuries.

2.2 Model description

TEM is a process-based, large-scale biogeochemical model that uses monthly climatic data and spatially explicit vegetation and soil information to simulate the dynamics of carbon and nitrogen fluxes and pool sizes of plants and soils (Raich et al., 1991; McGuire et al., 1992; Zhuang et al., 2010, 2015, 2020). However, in previous versions of TEM, the interactions between mosses and vascular plants on carbon and nitrogen cycling have not been included. Here we developed a TEM_Moss model by modifying model structure and incorporating activities of moss into extant TEM 5.0 (Zhuang et al., 2003). Based on the structure of TEM 5.0, we added carbon and nitrogen pools and fluxes to simulate activities of moss including photosynthesis, respiration, litterfall and nutrient and water cycling (Figure 1). Thus, the structure of TEM_Moss includes the processes of both vascular plants and mosses (Figure 1).

In TEM_Moss, moss photosynthesis (GPP_m) is described as a maximum rate, reduced by influence of photosynthetically active radiation, mean air temperature, mean atmospheric carbon

dioxide concentrations, moss moisture, and indirectly, nitrogen availability (Frolking et al., 1996;

Launiainen et al., 2015; Zhuang et al., 2002). For each time step, GPP_m is calculated as:

$$GPP_m = C_{max} * f(PAR) * f(T) * f(w_m) * f([CO_2]) * f(NA) \quad (1)$$

where C_{max} denotes the maximum rate of carbon assimilation by moss (units: g C m^{-2}mon^{-1}),

$f(PAR)$ is a scalar function that depends on monthly photosynthetically active radiation (PAR),

which is calculated as (Frolking et al., 1996; Launiainen et al., 2015; Kulmala et al., 2011):

$$f(PAR) = \frac{PAR}{b+PAR} \quad (2)$$

where b (units: μmol m^{-2} s^{-1}) is the half saturation constant for PAR use by moss as indicated by

the Michaelis–Menten kinetic.

The temperature effect on moss photosynthesis is modeled as a multiplier (Frolking et al.,

1996; Raich et al., 1991):

$$f(T) = \frac{(T-T_{min})*(T-T_{max})}{(T-T_{min})*(T-T_{max})-(T-T_{opt})^2} \quad (3)$$

where T is the monthly mean air temperature (units: $^{\circ}$C), and T_{min}, T_{max}, and T_{opt} are parameters

(units: $^{\circ}$C) that limit $f(T)$ to a range of zero to one.

The moisture effect is also modeled as a multiplier (Frolking et al., 1996; Raich et al.,

1991):

$$f(w_m) = \frac{(w_m-w_{min})*(w_m-w_{max})}{(w_m-w_{min})*(w_m-w_{max})-(w_m-w_{opt})^2} \quad (4)$$

where w_m is moss moisture (units: mm), and w_{min}, w_{max}, and w_{opt} are related parameters (units:

mm) that limit $f(w_m)$ to a range of zero to one.

149        $f([CO_2])$ is also a scalar function that depends on monthly mean atmospheric carbon

150   dioxide concentration (Zhuang et al., 2002; Raich et al., 1991):

151
$$f([CO_2]) = \frac{[CO_2]}{k_m + [CO_2]} \qquad (5)$$

152   where $[CO_2]$ (units: μL/L) represents monthly mean atmospheric carbon dioxide concentration,

153   the k_m (units: μL/L) is the internal CO_2 concentration at which moss C assimilation proceeds at

154   one-half its maximum rate.

155   The function $f(NA)$ models the limiting effects of plant nitrogen status on GPP (McGuire

156   et al., 1992; Zhuang et al., 2002), which is a scalar function that depends on monthly N available

157   for incorporation into plant production of new tissue.

158   Meanwhile, in TEM_Moss, we defined the moss respiration rate (R_m) as a function of

159   moss respiration rate at 10 °C, moss respiration temperature sensitivity which was expressed as a

160   Q_{10} function, and moss moisture (Launiainen et al., 2015; Frolking et al., 1996):

161
$$R_m = R_{10,m} * Q_{10,m}^{\frac{T_m - 10}{10}} * f^*(w_m) \qquad (6)$$

162   where $R_{10,m}$ (units: g C m^{-2}mon^{-1}) represents the moss respiration rate at 10 °C, the parameter

163    $Q_{10,m}$ is moss respiration temperature sensitivity, T_m is moss temperature (°C) and w_m is moss

164   moisture (mm).

165   The function $f^*(w_m)$ denotes the moisture effect on moss respiration. Here we used

166    $f^*(w_m)$ to distinguish with the function $f(w_m)$, which is moisture effect on moss

167   photosynthesis as mentioned earlier. $f^*(w_m)$ is defined as (Frolking et al., 1996; Zhuang et al,

168   2002):

169
$$f^*(w_m) = 1 - \frac{(w_m - w_{min} - w_{opt,r})^2}{(w_m - w_{min}) * w_{opt,r} + w_{opt,r}^2} \qquad (7)$$

170   where $w_{opt,r}$ (units: mm) denotes the optimal water content for moss respiration.

171   Besides, the carbon in litter production from mosses to soil ($L_{C,m}$) is modeled as

172   proportional to moss carbon biomass with a constant ratio (Zhuang et al., 2002):

173
$$L_{C,m} = cfall_m * MOSSC \qquad (8)$$

174   where MOSSC denotes the moss carbon biomass, and $cfall_m$ is the corresponding constant

175   proportion.

176   Thus, the change of moss carbon pool (MOSSC) can be modeled as:

177
$$\frac{dMOSSC}{dt} = GPP_m - R_m - L_{C,m} \qquad (9)$$

178   On the other hand, researches have shown that mosses can uptake substantial inorganic

179   nitrogen from the bulk soil (Ayres et al., 2006, Fritz et al., 2014). In our model, nitrogen uptake

180   by moss ($Nuptake_m$) is modelled as a function of available soil nitrogen, moss moisture, and

181   mean air temperature, and the relative amount of energy allocated to N versus C uptake (Zhuang

182   et al., 2002; Raich et al., 1991):

183
$$Nuptake_m = N_{max} * \frac{K_s * N_{av}}{k_n + K_s * N_{av}} * e^{0.0693T} * (1 - A_m) \qquad (10)$$

184   Where N_{max} is the maximum rate of nitrogen uptake by mosses (units: g C m^{-2}mon^{-1}), and N_{av}

185   (units: g m^{-2}) represents available soil nitrogen, which is treated as a state variable in our model.

186   k_n(units: g m^{-2}) is the concentration of available soil nitrogen at which nitrogen uptake proceeds

187   at one-half its maximum rate. T is the monthly mean air temperature (°C), and A_m is a unitless

188   parameter ranging from 0 to 1, which represents relative allocation of effort to carbon vs.

189   nitrogen uptake. K_s is a parameter accounting for relative differences in the conductance of the

190   soil to N diffusion, which can be calculated through moss moisture (Zhuang et al., 2002; Raich et

191   al., 1991):

192
$$K_s = 0.9 * \left(\frac{w_m}{w_f}\right)^3 + 0.1 \qquad (11)$$

193   where w_f (units: mm) denotes the moss field capacity.

194   The nitrogen in litter production from mosses to soil ($L_{N,m}$) is modeled as proportional to

195   moss nitrogen biomass with a constant ratio (Zhuang et al., 2002):

196
$$L_{N,m} = nfall_m * MOSSN \qquad (12)$$

197   where $nfall_m$ is the constant proportion to moss nitrogen biomass (MOSSN).

198   Thus, the changes in moss nitrogen pool (MOSSN) can be modeled as:

199
$$\frac{dMOSSN}{dt} = Nuptake_m - L_{N,m} \qquad (13)$$

200   At the same time, total carbon and nitrogen in litterfall, and total nitrogen uptake from

201   soil available nitrogen are changed due to incorporation of mosses:

202
$$Litterfall_C = L_{C,v} + L_{C,m} \qquad (14)$$

203
$$Litterfall_N = L_{N,v} + L_{N,m} \qquad (15)$$

204
$$Nuptake = Nuptake_v + Nuptake_m \qquad (16)$$

205   Where $L_{C,v}$ and $L_{N,v}$ are carbon and nitrogen in litter production from vascular plants to soil, and

206    $Nuptake_v$ is nitrogen uptake by vascular plants (Raich et al., 1991; Melillo et al., 1993; Zhuang

207   et al., 2003).

208   Except above equations, other governing equations in TEM 5.0 have not been changed.

209 More equations of TEM 5.0 have been documented in previous studies (Raich et al., 1991;

210 McGuire et al., 1992; Zhuang et al., 2003; Zha and Zhuang, 2018).

211   In TEM 5.0, a soil thermal module (STM) simulates soil thermal dynamics considering

212 the effects of moss thickness, soil moisture, and snowpack (Zhuang et al., 2001, 2002). In STM,

213 soil profile was treated as a three soil-layer system: (1) a moss plus fibric soil organic layer, (2) a

214 humic organic soil layer, and (3) a mineral soil layer, and temperature for each layer can be

215 derived from STM (Zhuang et al., 2001, 2002, 2003). Temperature in moss layer is estimated

216 with STM.

217   A water balance module (WBM) was also incorporated into TEM 5.0 to simulate soil

218 hydrologic dynamics (Vörösmarty et al., 1989; Zhuang et al., 2001). The WBM receives

219 information on precipitation, air temperature, potential evapotranspiration, vegetation, soils and

220 elevation to predict soil moisture evapotranspiration and runoff (Vörösmarty et al., 1989). The

221 whole soil was treated as a single profile in WBM (Vörösmarty et al., 1989; Zhuang et al., 2001).

222 To simulate moss moisture, we added a moss layer on the soil profile by modifying the WBM

223 (Figure 2). Similar to soil moisture, moss moisture is also treated as a state variable in the revised

224 WBM, which is modeled as:

225   $\frac{dw_m}{dt} = \text{snowfall} + \text{rainfall} - \text{percolation} - \text{moss evapotranspiration}$   (17)

226 where the term "percolation" denotes the percolation from moss, which is the sum of rainfall

227 percolation and snowmelt percolation from moss. We assume that there is no runoff from moss

228 layer.

229 Accompanied by the above equation, changes in soil water (SM) is modified as:

230 $$\frac{dSM}{dt} = \text{percolation} - \text{rain excess} - \text{snow excess} - \text{plant evapotranspiration} \qquad (18)$$

231 Calculations for these water fluxes regarding vascular plants were not changed. More details

232 about an earlier version of WBM were described in Vörösmarty et al. (1989) and Zhuang et al.

233 (2001).

2.3 Model parameterization and validation

235   The newly introduced parameters that are associated with moss activities were documented

236 in Table 1. We parameterized the TEM_Moss for six representative ecosystem types in northern

237 high latitudes with gap-filled monthly net ecosystem productivity (NEP, g $Cm^{-2}mon^{-1}$) data from

238 the AmeriFlux network (Davidson et al., 2000). We assumed that the moss types are associated

239 with the representative ecosystem types, which means we tuned the moss-related parameters for

240 the six representative ecosystem types. Except for the moss-related parameters, other parameters

241 related to vascular plants are default based on Zha and Zhuang, 2018. The information of six sites

242 that we chose to calibrate the TEM_Moss was compiled in Table 2. The parameterization was

243 conducted using a global optimization algorithm known as SCE-UA (Shuffled complex evolution)

244 method, which aims to minimize the difference between model simulations and measurements

245 (Duan et al., 1994). In our calibration, the cost function of the minimization is:

246 $$\text{Obj} = \sum_{i=1}^{k}(\text{NEP}_{obs,i} - \text{NEP}_{sim,i})^2 \qquad (19)$$

247 Where $\text{NEP}_{obs,i}$ and $\text{NEP}_{sim,i}$ are the measured and simulated NEP, respectively. k is the number

248 of data pairs for comparison. Fifty independent sets of parameters were converged to minimize the

249 objective function, and finally the optimized parameters were derived as the mean of these 50 sets

250 of inversed parameters. We presented the boxplot of parameter posterior distributions at sites

251 chosen for calibration (Figure 5). At the same time, the results of model parameterization were

252   shown in Figure 3. Besides these parameters related to moss, all other parameters use their default

253   values in TEM 5.0 (Zhuang et al., 2003). Note, in TEM 5.0 and its application, the parameters

254   were also calibrated for each representative ecosystem in northern high latitudes. Specifically,

255   TEM 5.0 was parameterized for mixed grassland/sub-shrublands, moist non-acidic tundra, mixed

256   hardwood and conifer forests, tallgrass prairie, savanna tropical forests, tussock tundra, and conifer

257   forest in the region. TEM 5.0 was then extrapolated to the region to quantify carbon dynamics

258   without considering the role of moss in boreal ecosystems (Zhuang et al., 2003). Here our revised

259   model TEM_Moss was parameterized for representative ecosystems in the region by explicitly

260   considering the role of moss in soil physics and carbon and nitrogen dynamics. The TEM_Moss

261   optimized parameters were then used for model validation and extrapolation as well as comparison

262   with TEM 5.0 simulations.

263   We verified the TEM_Moss simulated NEP, soil moisture and soil temperature. First, we

264   conducted site-level simulations at six sites that contain level-4 gap-filled monthly NEP data from

265   the AmeriFlux network (Table 3). Site-level monthly gap-filled soil moisture and soil temperature

266   data were organized from the ORNL DAAC Dataset (https://daac.ornl.gov/) to make comparison

267   with model simulations (Table 4 and Table 5). Local climate data including monthly air

268   temperature ($^{\circ}$C), precipitation (mm), and cloudiness (%) were obtained to drive these model

269   simulations.

270   **2.4 Regional Extrapolation**

271   With six site-level calibrated parameters, TEM-Moss is applied to the region pixel by pixel based

272   on vegetation distribution data. Both TEM_Moss and TEM 5.0 were applied to northern high

273   latitudes (above 45 °N) for historical (the 20th century) and future (the 21st century) quantifications

274   on carbon dynamics. For historical simulations, climatic forcing data including monthly air

275 temperature, precipitation, and cloudiness and atmospheric CO_2 concentrations during the 20th

276 century, were collected from the Climatic Research Unit (CRU TS3.1) from the University of East

277 Anglia (Harris et al., 2014). Other ancillary inputs including gridded soil texture (Zhuang et al.,

278 2015), elevation (Zhuang et al., 2015), and potential natural vegetation (Melillo et al., 1993) were

279 also organized. For future simulations, two contrasting Intergovernmental Panel on Climate

280 Change (IPCC) climate scenarios (RCP 2.6 and RCP 8.5) were used to drive the models. The future

281 climate forcing data and atmospheric CO_2 concentrations during the 21st century under these two

282 climate change scenarios were derived from the HadGEM2-ESmodel, which is a member of

283 CMIP5project213 (https://esgf-node.llnl.gov/search/cmip5/, January 2017).

284   Simulations were conducted at a spatial resolution of 0.5° latitude × 0.5° longitude (Zhuang

285 et al., 2001, 2002). A spin-up was run to reach an equilibrium for each pixel, and the values of state

286 variables at equilibrium were treated as initial values for transient simulations (McGuire et al.,

287 1992). Specifically, we chose the first 30 years in the whole 100-year climatic forcing data to spin-

288 up the models when conducting historical and future simulations. For each of the simulations, net

289 primary production (NPP), heterotrophic respiration (R_H), and net ecosystem production (NEP)

290 were analyzed. We denoted that a positive NEP represents a CO_2 sink from the atmosphere to

291 terrestrial ecosystems, while a negative value represents a source of CO_2 from terrestrial

292 ecosystems to the atmosphere.

293   In these simulations, for each pixel, we assumed its moss distribution area is the same as

294 the vascular plant distribution. The total carbon uptake/emission of mosses in a pixel are calculated

295 as the multiplication of pixel area with the carbon fluxes such as NEP (units: g C m^{-2} $month^{-1}$).

296 Moss-related parameters for representative ecosystems are calibrated (Fig. 4 and Table 1) or

297 obtained from previous model parameterization and the rest of model parameters are default from

298 Zha and Zhuang (2018).

3. Results

3.1 Model Validation

301   TEM_Moss was able to reproduce the monthly NEP and performed better than TEM 5.0

302 at chosen sites, with larger R-square values and smaller RMSE (Figure 6, Table 6). R-square for

303 TEM_Moss reached 0.94 at Bartlett Experimental Forest site and 0.72 at Ivotuk site (Table 6). R-

304 square values for TEM 5.0 showed a similar pattern, reaching 0.91 and with minimum value of

305 0.43 at Bartlett Experimental Forest and Ivotuk sites, respectively (Table 6). Except for Ivotuk

306 site, R-squares for TEM_Moss are all higher than 0.8 at the chosen sites, while most R-squares

307 for TEM 5.0 are from 0.62 to 0.75 (Table 6). On the other hand, RMSE for TEM_Moss is lower

308 than that for TEM 5.0 at each site (Table 6).

309   We presented the comparisons between measured and simulated volumetric soil moisture

310 (VSM) from TEM_Moss and TEM 5.0 (Figure 7). Statistical analysis shows that TEM_Moss

311 reproduces the soil moisture well with R-squares ranging from 0.51 at US-Bkg to 0.87 at US-Atq

312 (Table 7). R-squares for TEM_Moss are substantially higher than that for TEM 5.0 at most

313 chosen sites, except for US-Atq (Table 7). RMSE for TEM_Moss is lower than that for TEM 5.0

314 at each site (Table 7). Similarly, comparisons between measured and simulated soil temperature

315 at 5 cm depth (ST_5) from TEM_Moss and TEM 5.0 indicated that TEM_Moss can reproduce

316 the soil temperature with R-squares ranging from 0.81 at US-Ho1 to 0.91 at US-Bkg, while TEM

317 5.0 reproduces the soil temperature with R-squares ranging from 0.69 at BE-Vie to 0.89 at US-

318 Bkg (Figure 8; Table 8). Although R-squares for both models are relatively high and RMSE for

319   them are relatively low, TEM_Moss still shows higher R-squares and lower RMSE than TEM

320   5.0 (Table 8).

3.2 Regional carbon dynamics during the 20th century

322   Both TEM_Moss and TEM 5.0 were used to simulate northern high-latitude regional

323   carbon balance during the 20th century (Figure 9). Higher NEP was correlated with the

324   combination of relatively higher NPP and lower heterotrophic respiration (R_H). TEM_Moss

325   indicated that the northern high latitudes acted as a carbon sink of 221.9 Pg with an inter-annual

326   standard deviation of 0.31 Pg C yr^{-1} during the 20th century, which is 132.7 Pg larger than 89.2 Pg

327   simulated by TEM 5.0 (Figure 10). The simulated NEP by TEM_Moss ranges from 1.38 Pg C yr^{-1}

328   ^{1} to 3.05 Pg C yr^{-1}, while the range by TEM 5.0 was from 0.11 Pg C yr^{-1} to 1.75 Pg C yr^{-1} (Figure

329   9). The patterns of the simulated NEP from two models were similar, both showing a general

330   increasing trend throughout the 20th century (Figure 9). By 2000, the TEM_Moss simulation

331   indicated that the northern high-latitude region stored 3.05 Pg C yr^{-1}, which is more than twice as

332   the storage estimated by TEM 5.0 (1.33 Pg C yr^{-1}, Figure 9). Both models indicated that carbon

333   uptake by the northern ecosystems during the second half of the 20th century was higher than the

334   first half for most part of the region, and only a small portion of the region lost carbon in last

335   century (Figure 10).

336   Simulated total NPP by TEM_Moss was 9.6 Pg C yr^{-1}, ranging from 8.52 Pg C yr^{-1} to

337   10.65 Pg C yr^{-1} in the 20th century, with 1.69 Pg C yr^{-1} of moss NPP and 7.93 Pg C yr^{-1} of

338   vascular plants NPP (Figure 9). Moss NPP ranges from 1.23 Pg C yr^{-1} to 2.14 Pg C yr^{-1} and the

339   ratio of moss NPP to vascular plants NPP is 0.21 (Figure 9). TEM 5.0 estimated 0.8 Pg C yr^{-1}

340   lower total NPP than TEM_Moss, but 0.87 Pg C yr^{-1} higher NPP for vascular plants (Figure 9).

341   On the other hand, average heterotrophic respiration in the 20th century was 7.38 Pg C yr^{-1} and

342 all years were within about 5% of this value (Figure 9). TEM 5.0 projected 0.53 Pg C yr^{-1} higher

343 R$_H$ than TEM_Moss (7.91 Pg C yr^{-1}, Figure 9). Overall, TEM_Moss predicted higher total NPP

344 but lower R$_H$, which jointly caused a pronounced difference in NEP between two models.

345   Both models estimated that soil organic carbon and vegetation carbon were accumulating

346 continuously in the 20th century (Figure 11). TEM_Moss indicated that regional SOC and VEGC

347 accumulated 96.3 Pg C and 115.2 Pg C, respectively, and the carbon uptake by moss was 10.4 Pg

348 in the period (Figure 11, Table 10). As simulated by TEM_Moss, 43.4%, 51.9% and 4.7% of

349 total carbon uptake in the region was assimilated to soils, vascular plants and mosses,

350 respectively (Table 10). TEM 5.0 simulated that SOC increased by 31.7 Pg at the end of the 20th

351 century, which is 64.6 Pg C less than the value estimated by TEM_Moss (Table 10). TEM 5.0

352 estimated 57.7 Pg C in plants less than the value estimated by TEM_Moss (57.5 Pg C, Table 10).

353 35.5% and 64.5% of total carbon was as SOC and VEGC, respectively.

3.3 Regional carbon dynamics during the 21st century

355   Under the RCP 2.6 scenario, TEM_Moss simulated NEP of 2.07 Pg C yr^{-1} with the range

356 from 0.41 Pg C yr^{-1} to 3.2 Pg C yr^{-1}, and the inter-annual standard deviation of 0.59 Pg C yr^{-1}

357 during the 21st century (Figure 12 (a)). The regional sink shows a decreasing pattern in the 2000s

358 and then generally increases over the remaining years of the 21st century (Figure 12 (a)). For

359 comparison, TEM 5.0 predicted that the average NEP of 0.28 Pg C yr^{-1} with the range from -1.48

360 Pg C yr^{-1} to 1.69 Pg C yr^{-1} during the 21st century (Figure 12 (a)). Thus, TEM 5.0 projected 179.1

361 Pg C stored in northern ecosystems is less than the estimation from TEM_Moss in the 21st

362 century. Besides, TEM 5.0 simulated that the regional NEP showed a decreasing trend and the

363 region fluctuates between sinks and sources during the century (Figure 12 (a)). The spatial

364 patterns from two models also showed differences. TEM_Moss indicated that the region

365 accumulates carbon over this century, while TEM 5.0 simulated that some regions changed from

366 a carbon sink to a source in the second half of the century (Figure 13 (a)). Simulated regional

367 NPP by TEM_Moss ranges from 11.2 to 13.7 Pg C yr^{-1} with a mean of 12.98 Pg C yr^{-1} in this

368 century, while average NPP predicted by TEM 5.0 is 1.46 Pg C yr^{-1} lower than that value (11.52

369 Pg C yr^{-1} (Figure 12(a)). TEM_Moss simulated NPP has 3.74 Pg C yr^{-1} from moss and 9.24 Pg C

370 yr^{-1} from vascular plants, which account for 28.8% and 71.2% of total NPP, respectively (Figure

371 12(a)). Meanwhile, TEM_Moss estimated that R_H is 10.91 Pg C yr^{-1}, while TEM 5.0 predicted it

372 as 11.24 Pg C yr^{-1}, which is higher (Figure 12(b)). Both models projected that soil organic carbon

373 and vegetation carbon accumulate in this century but with different magnitudes (Figure 14 (a)).

374 TEM_Moss predicted that regional SOC and VEGC accumulated 84.7 Pg C and 112.6 Pg C,

375 respectively, during the 21st century, while TEM 5.0 predicted that a smaller increase with 12.1

376 and 15.5 Pg C in SOC and VEGC, respectively (Figure 14 (a), Table 12 (a)). Besides,

377 TEM_Moss also predicted an increasing of 9.4 Pg C in MOSSC, accounting for 4.5% of the total

378 carbon uptake in this region (Table 12(a)).

379   Under the RCP 8.5 scenario, TEM_Moss simulated annual NPP of 13.84 Pg C yr^{-1} with a

380 range from 11.09 to 16.94 Pg C yr^{-1}, which is 1.31 Pg C yr^{-1} higher than the projection from

381 TEM 5.0 (Figure 12 (b)). Total NPP estimated by TEM_Moss has 3.84 Pg C yr^{-1} from moss and

382 10 Pg C yr^{-1} from vascular plants (Figure 12(b)). Annual R_H was 11.28 Pg C yr^{-1} estimated by

383 TEM_Moss and 11.54 Pg C yr^{-1} by TEM 5.0, respectively (Figure 12(b)). Consequently,

384 TEM_Moss projected NEP was 2.56 Pg C yr^{-1} with the inter-annual standard deviation of 0.93

385 Pg C yr^{-1} in this century (Figure 12(b)). NEP ranges from 0.67 Pg C yr^{-1} to 4.78 Pg C yr^{-1}

386 estimated with TEM_Moss, while from -1.69 Pg C yr^{-1} to 2.65 Pg C yr^{-1} with a mean of 0.99 Pg

387 C yr^{-}1 was estimated by TEM 5.0 (Figure 12(b)). TEM_Moss predicted more carbon uptake of

388 157.5 Pg than TEM 5.0 during the 21st century. Both models predicted that NEP showed an

389 increasing trend during the 21st century (Figure 12(b)). Moreover, similar spatial patterns of

390 carbon sinks and sources appeared in the projections from two models (Figure 13(b)). Soil

391 organic carbon and vegetation carbon shows an increasing trend from both models (Figure

392 14(b)). Regional SOC and VEGC increased by 92.5 Pg C and 153.6 Pg C, respectively by the

393 end of the 21st century predicted by TEM_Moss. In contrast, the increase of 44.2 Pg C and 54.5 Pg

394 C of SOC and VEGC, respectively, was predicted by TEM 5.0 (Figure 14(b), Table 12 (b)).

395 TEM_Moss predicted an increase of 10.1 Pg C in MOSSC (Table 12(b)).

396 **4. Discussion**

397 **4.1 The role of moss in the regional carbon dynamics**
398
399   Global warming has been pronounced in recent decades, particularly at high latitudes

400 (IPCC, 2014; Tape et al., 2006; Stow et al., 2004). An enormous amount of soil organic carbon

401 stored in northern high-latitude regions (Tarnocai et al., 2009; Schuur et al., 2008) is expected to

402 affect a broad spectrum of ecological and human systems, and cause rapid changes in the Earth

403 system when undergoing substantial climate change (Serreze and Francis 2006; Davidson and

404 Janssens, 2006; McGuire et al., 2009). Improving projections for carbon budget of high latitude

405 terrestrial ecosystems is essential for understanding global carbon–climate feedbacks (Melillo et

406 al., 2011; Todd-Brown et al., 2013).

407   Our simulations suggest that mosses play an important role in the regional carbon

408 dynamics, which is consistent with previous studies (McGuire et al., 2009; Turetsky et al., 2012).

409 First of all, mosses are productive with carbon assimilation even during low temperature, water

410 content and irradiance (Kallio and Heinonen, 1975; Harley et al., 1989). For example, mosses

411 can tolerate drought through physiological responses, such as by suspending metabolism and by

412   withstanding cell dessication (Turetsky et al., 2012; Oechel and Van Cleve, 1986). The key

413   functional traits related to water, nutrient, and thermal tolerances of mosses enable them to fit in

414   harsh northern conditions (Shetler et al., 2008; Turetsky et al., 2012). Thus, with incorporation of

415   moss into our models, the total NPP estimation in our model is affected. Mosses also act as a

416   powerful competitor with vascular plants for nutrient uptake. Their rapid nutrient acquisition and

417   slow nutrient loss through slow decomposition may constrain concentrations of plant-available

418   nitrogen (Hobbie et al., 2000; Turetsky et al., 2010; Oechel and Van Cleve, 1986; Gornall et al.,

419   2007), which will further decrease NPP of vascular plants. Our model results suggested that the

420   NPP of vascular plants considering moss is indeed lower than previous NPP estimates without

421   considering moss, but the total NPP is larger than before. We estimated that mosses contribute

422   17.6% of NPP in the 20th century, and 28.8% and 27.6% in the 21st century under the RCP 2.6

423   and RCP 8.5 scenarios, respectively. This is comparable with the results reported by a synthesis

424   study, indicating an average contribution 20% of aboveground NPP from moss in upland boreal

425   forests and the contribution is 48% in wetlands ecosystems. Frolking et al. (1996) even reported

426   a contribution of 38.4% to total NPP by moss at a boreal forest site. Moreover, mosses can also

427   influence heterotrophic respiration (R_H) through their effects on soil thermal and hydrologic

428   dynamics (Zhuang et al., 2001). With the layer of moss, soil temperature tends to decrease but

429   soil moisture tends to increase (Oechel and Van Cleve, 1986), which will further decrease soil

430   respiration in summer. This supports our results that TEM_Moss simulated R_H is lower than that

431   by TEM 5.0. With a combination of higher NPP and lower R_H, NEP predicted by TEM_Moss is

432   larger than that by TEM 5.0. The two contrasting regional simulations by TEM_Moss and TEM

433   5.0 indicated the region is currently a carbon sink, which is consistent with previous studies

434   (White et al., 2000; McGuire et al., 2009; Schimel et al., 2001). Our study estimates that regional

435   NEP during the 20th century is 2.2 Pg C yr^{-1} by TEM_Moss and 0.89 Pg C yr^{-1} by TEM 5.0,

436   respectively. In the 1990s, the regional sink is projected to be 2.7 and 1.1 Pg C yr^{-1} by

437   TEM_Moss and TEM 5.0 respectively. Compared with other existing studies, our regional

438   estimates of NEP are within the reasonable range from other existing studies. McGuire et al.

439   (2009) estimated a land sink of 0.3–0.6 Pg C yr^{-1} for the pan-arctic region for the 1990s, which is

440   closer to our estimation by TEM 5.0 but less than the projection by TEM_Moss. The top-down

441   atmospheric analyses indicate that the sink of pan-arctic region is between 0 and 0.8 Pg C yr^{-1} in

442   the 1990s (Menon et al. 2007). Besides, Schimel et al. (2001) reported an estimation of the

443   northern extratropical NEP is from 0.6 to 2.3 Pg C yr^{-1} in the late 20th century, which is

444   comparable to our estimates. Our simulations also confirmed that mosses and vascular plants

445   respond to climate change similarly in terms of their productivity (Turetsky et al. 2010).

446   **4.2 Model Uncertainty and limitations**

447   There are a number of uncertainty sources in our model simulations. First, due to the

448   limited understanding of moss photosynthesis (He et al., 2015) and various moss N uptake

449   pathways (e.g., Bay et al 2013; Berg et al 2013), a few important assumptions have been made in

450   our modeling. For instance, we assume that mosses behave similarly to vascular plants regarding

451   photosynthesis and soil N uptake is the only pathway for mosses without considering N uptake

452   through N fixers and atmospheric wet N deposition (Ayres et al. 2006). Second, the errors in the

453   observed data will influence our parameterization results, which will bias our regional estimates

454   of carbon dynamics. Second, climatic driving data are also a source of uncertainty for historical

455   and future simulations. Third, model assumptions will also induce additional uncertainties. For

456   instance, we assumed that vegetation distribution will remain unchanged during the transient

457   simulation. However, vegetation will change in response to warming climate and disturbances

458   such as fire and insect outbreaks in the region (Hansen et al., 2006), which will affect carbon

459   budget. Missing potential responses to disturbances in our model shall introduce additional

460   uncertainties (Soja et al. 2007; Kasischke and Turetsky, 2006). Future moss dynamics will also

461   impact carbon dynamics in this region. For instance, a long-term warming experiments along

462   natural climatic gradients, ranging from Swedish subarctic birch forest and subarctic/subalpine

463   tundra to Alaskan arctic tussock tundra concluded that both diversity and abundance of mosses

464   are likely to decrease under arctic climate warming (Long et al. 2012). Similarly, total moss

465   cover declined in both heath and mesic meadow under experimental long-term warming (by 1.5–

466   3 °C), driven by general declines in many species (Alatalo et al., 2020).   Due to global warming,

467   significant losses in moss diversity are expected in boreal forests and alpine biomes, leading to

468   changes in ecosystem structure and function, nutrient cycling, and carbon balance (He et al.,

469   2015).

470   We conducted ensemble regional simulations with 50 sets of parameters to quantify

471   model uncertainty due to uncertain parameters. The 50 sets of parameters were obtained using

472   the method in Tang and Zhuang (2008). The ensemble means and the inter-simulation standard

473   deviations are used to measure the model uncertainty (Figure 15). TEM_Moss predicted that the

474   regional cumulative carbon ranges from a carbon loss of 266 Pg C to a carbon sink of 567.3 Pg C

475   by different ensemble members, with a mean of 161.1±142.1 Pg during the 21st century under the

476   RCP 2.6 scenario. Under the RCP 8.5 scenario, TEM_Moss predicted that the region acts from a

477   carbon source of 79.1 Pg C to a carbon sink of 625.9 Pg C, with a mean of 186.7±166.1 Pg

478   during the 21st century (Figure 15).

479   This study took an important step to incorporate moss into an extant ecosystem model

480   that has not explicitly consider the role of moss and its interactions with vascular plants. Our

481   model simulations showed that mosses have strong influences on regional ecosystem carbon

482   cycling, by affecting the soil thermal, nitrogen availability, and water conditions of terrestrial

483   ecosystems. However, there are still limitations in our model. First, we did not differentiate

484   various kinds of mosses because they have their own functional traits. Different kinds of mosses

485   may provide different levels of insulation for soil, resulting in different soil thermal conditions

486   that affect microbial activities. The structural and physiological traits of mosses will differ

487   largely in different moss groups, such as feather moss versus Sphagnum (Turetsky et al., 2010).

488   In addition, we lack spatially explicit information of moss distribution in the region, which will

489   lead to a large regional uncertainty of carbon quantification. We assumed that moss area

490   distribution is the same as its associated vegetation distribution. Another limitation is that some

491   important physiological traits of moss have not been modeled. For example, moss abundance

492   may change following shifts in vascular species composition due to shading or burial by vascular

493   litter (Turetsky et al., 2010; Cornelissen et al., 2007). Furthermore, disturbance such as wildfires

494   can also influence moss activities.

495   **5. Conclusions**

496   This study explicitly incorporated moss into an extant process-based terrestrial ecosystem model

497   to investigate the carbon dynamics in the Arctic for present day and future. Historical regional

498   simulations with TEM_Moss indicated that the region is a carbon sink of 221.9 Pg C over the 20th

499   century, and this sink may decrease to 206.7 Pg C under the RCP 2.6 scenario or increase to 256.2

500   Pg C under the RCP 8.5 scenario during the 21st century. Compared with an earlier version of TEM

501   that has not explicitly modeled moss, TEM_Moss projected that the region stored 132.7 Pg more

502   C over the last century, 179.1 Pg and 157.5 Pg more C under the RCP 2.6 and RCP 8.5 scenarios,

503   respectively. This study demonstrated that moss activities have large effects on ecosystem soil

504 thermal, water, and carbon dynamics through their interactions with vascular plants. This study

505 highlights the importance of considering the moss dynamics in Earth System Models to adequately

506 quantify the carbon–climate feedbacks in the Arctic.

6. Acknowledgments

508 This research was supported by an NSF project (IIS-1027955), a DOE project (DE-SC0008092),

509 and a NASA LCLUC project (NNX09AI26G). We acknowledge the Rosen High Performance

510 Computing Center at Purdue for computing support. We also acknowledge the World Climate

511 Research Programme's Working Group on Coupled Modeling Intercomparison Project CMIP5,

512 and we thank the climate modeling groups for producing and making available their model

513 output. The data of this study can be accessed from Purdue Research Repository.

514

References

516 Allison, S. D., and Treseder, K. K.: Warming and drying suppress microbial activity and carbon cycling in

517 boreal forest soils, Global change biology, 14, 2898-2909, 10.1111/j.1365-2486.2008.01716.x, 2008.

518 Basilier, K.: Moss-associated nitrogen fixation in some mire and coniferous forest environments around

519 Uppsala, Sweden, Lindbergia, 5, 84-88, 1979.

520 Bay, G., Nahar, N., Oubre, M., Whitehouse, M.J., Wardle, D.A., Zackrisson, O., Nilsson, M.-C. and

521 Rasmussen, U. (2013), Boreal feather mosses secrete chemical signals to gain nitrogen. New Phytol, 200:

522 54-60. https://doi.org/10.1111/nph.12403

523 Ben Bond-Lamberty, S. T. G., Douglas E. Ahl and Peter E. Thornton: Reimplementation of the Biome-

524 BGC model to simulate successional change, Tree Physiology, 25, 413–424, 2005.

525 Berg, Andreas, et al. "Transfer of Fixed-N from N_2-Fixing Cyanobacteria Associated with the Moss

526 Sphagnum Riparium Results in Enhanced Growth of the Moss." Plant and Soil, vol. 362, no. 1/2, 2013,

527 pp. 271–278. JSTOR, www.jstor.org/stable/42951898. Accessed 28 May 2021.

528 Bond-Lamberty, B., Peckham, S. D., Ahl, D. E., and Gower, S. T.: Fire as the dominant driver of central

529 Canadian boreal forest carbon balance, Nature, 450, 89-92, 10.1038/nature06272, 2007.

530 Bond-Lamberty, B., and Thomson, A.: Temperature-associated increases in the global soil respiration

531 record, Nature, 464, 579-582, 10.1038/nature08930, 2010.

Burke, E. J., Ekici, A., Huang, Y., Chadburn, S. E., Huntingford, C., Ciais, P., Friedlingstein, P., Peng, S. & Krinner, G. 2017. Quantifying uncertainties of permafrost carbon-climate feedbacks. *Biogeosciences,* 14**,** 3051-3066.

Cahoon, S. M., Sullivan, P. F., Shaver, G. R., Welker, J. M., Post, E., and Holyoak, M.: Interactions among shrub cover and the soil microclimate may determine future Arctic carbon budgets, Ecology letters, 15, 1415-1422, 10.1111/j.1461-0248.2012.01865.x, 2012.

Chadburn, S. E., Burke, E. J., Cox, P. M., Friedlingstein, P., Hugelius, G., and Westermann, S.: An observation-based constraint on permafrost loss as a function of global warming, Nature Climate Change, 7, 340-344, 10.1038/nclimate3262, 2017.

Charles J. Vörösmarty, B. M. I., Annette L. Grace, and M. Patricia Gildea: Continental scale models of water balance and fluvial transport: an application to South America, Global biogeochemical cycles, 3, 241-265, 1989.

Christian Fritz, L. P. M. L., Muhammad Riaz, Leon J. L. van den Berg, Theo J. T.M. Elzenga: Sphagnum Mosses - Masters of Efficient N-Uptake while Avoiding Intoxication, PLoS ONE, 9, 10.1371/journal.pone.0079991, 2014.

Clarke, G. C. S.: Productivity of Bryophytes in Polar Regions, Annals of botany, 35, 99–108, 1971.

Collins, W. C. O. a. N. J.: Comparative COz exchange patterns in mosses from two tundra habitats at Barrow, Alaska, Canadian Journal of Botany, 54, 1355-1369, 1976.

Comyn-Platt, E., Hayman, G., Huntingford, C., Chadburn, S. E., Burke, E. J., Harper, A. B., Collins, W. J., Webber, C. P., Powell, T., Cox, P. M., Gedney, N. & Sitch, S. 2018. Carbon budgets for 1.5 and 2 °C targets lowered by natural wetland and permafrost feedbacks. *Nature Geoscience,* 11**,** 568-573.

Cornelissen, J. H., Lang, S. I., Soudzilovskaia, N. A., and During, H. J.: Comparative cryptogam ecology: a review of bryophyte and lichen traits that drive biogeochemistry, Annals of botany, 99, 987-1001, 10.1093/aob/mcm030, 2007.

Davidson, E. A., Trumbore, S. E., and Amundson, R.: Soil warming and organic carbon content, Nature, 408, 789, 10.1038/35048672, 2000.

Davidson, E. A., and Janssens, I. A.: Temperature sensitivity of soil carbon decomposition and feedbacks to climate change, Nature, 440, 165-173, 10.1038/nature04514, 2006.

Davidson, E. A., Janssens, I. A., and Luo, Y.: On the variability of respiration in terrestrial ecosystems: moving beyond Q10, Global change biology, 12, 154-164, 10.1111/j.1365-2486.2005.01065.x, 2006.

DeLuca, T. H., Zackrisson, O., Gentili, F., Sellstedt, A., and Nilsson, M. C.: Ecosystem controls on nitrogen fixation in boreal feather moss communities, Oecologia, 152, 121-130, 10.1007/s00442-006-0626-6, 2007.

565 Duan, Q., Sorooshian, S., and Gupta, V. K.: Optimal use of the SCE-UA global optimization method for
566 calibrating watershed models, Journal of Hydrology, 158, 265-284, 1994.

567 E. S. Euskirchen, A. D. M., F. S. Chapin, III, S. Yi, and C. C. Thompson: Changes in vegetation in
568 northern Alaska under scenarios of climate change, 2003–2100: implications for climate feedbacks,
569 Ecological Applications, 19, 1022–1043, 2009.

570 Edward A. G. Schuur, J. B., Josep G. Canadell, Eugenie Euskirchen, Christopher B., Field, S. V. G.,
571 Stefan Hagemann, Peter Kuhry, Peter M. Lafleur, Hanna Lee, Galina, Mazhitova, F. E. N., Annette Rinke,
572 Vladimir E. Romanovsky, Nikolay Shiklomanov, and Charles Tarnocai, S. V., Jason G. Vogel, And Sergei
573 A. Zimov: Vulnerability of Permafrost Carbon to Climate Change: Implications for the Global Carbon
574 Cycle, BioScience, 58, 701-714, 2008.

575 Edward Ayres, R. v. d. W., Martin Sommerkorn, Richard D. Bardgett: Direct uptake of soil nitrogen by
576 mosses, Biology Letters, 2, 286-288, 10.1098/rsbl.2006.0455, 2006.

577 Esteban G. Jobbágy, and Jackson, R. B.: The vertical distribution of soil organic carbon and its relation to
578 climate and vegetation, Ecological applications, 10, 423-436, 2000.

579 Frolking, S., Roulet, N. T., Tuittila, E., Bubier, J. L., Quillet, A., Talbot, J., and Richard, P. J. H.: A new
580 model of Holocene peatland net primary production, decomposition, water balance, and peat
581 accumulation, Earth System Dynamics, 1, 1-21, 10.5194/esd-1-1-2010, 2010.

582 Gilmanov, T. G., Tieszen, L. L., Wylie, B. K., Flanagan, L. B., Frank, A. B., Haferkamp, M. R., Meyers,
583 T. P., and Morgan, J. A.: Integration of CO_2 flux and remotely-sensed data for primary production and
584 ecosystem respiration analyses in the Northern Great Plains: potential for quantitative spatial
585 extrapolation, Global Ecology and Biogeography, 14, 271-292, 10.1111/j.1466-822X.2005.00151.x, 2005.

586 Gornall, J. L., Jonsdottir, I. S., Woodin, S. J., and Van der Wal, R.: Arctic mosses govern below-ground
587 environment and ecosystem processes, Oecologia, 153, 931-941, 10.1007/s00442-007-0785-0, 2007.

588 Gornall, J. L., Woodin, S. J., Jonsdottir, I. S., and van der Wal, R.: Balancing positive and negative plant
589 interactions: how mosses structure vascular plant communities, Oecologia, 166, 769-782,
590 10.1007/s00442-011-1911-6, 2011.

591 Gough, C. M., Hardiman, B. S., Nave, L. E., Bohrer, G., Maurer, K. D., Vogel, C. S., Nadelhoffer, K. J.,
592 and Curtis, P. S.: Sustained carbon uptake and storage following moderate disturbancein a Great Lakes
593 forest, Ecological Applications, 23, 1202-1215, 2013.

594 Goulden, M. L., Winston, G. C., McMillan, A. M. S., Litvak, M. E., Read, E. L., Rocha, A. V., and Rob
595 Elliot, J.: An eddy covariance mesonet to measure the effect of forest age on land atmosphere exchange,
596 Global change biology, 12, 2146-2162, 10.1111/j.1365-2486.2006.01251.x, 2006.

597 Hansen, J., Sato, M., Ruedy, R., Lo, K., Lea, D. W., and Medina-Elizade, M.: Global temperature change,

598 Proceedings of the National Academy of Sciences of the United States of America, 103, 14288-14293,

599 10.1073/pnas.0606291103, 2006.

600 Harris, I., Jones, P. D., Osborn, T. J., and Lister, D. H.: Updated high-resolution grids of monthly climatic

601 observations - the CRU TS3.10 Dataset, International Journal of Climatology, 34, 623-642,

602 10.1002/joc.3711, 2014.

603 Hayes, D. J., McGuire, A. D., Kicklighter, D. W., Gurney, K. R., Burnside, T. J., and Melillo, J. M.: Is the

604 northern high-latitude land-based CO2 sink weakening?, Global Biogeochemical Cycles, 25, n/a-n/a,

605 10.1029/2010gb003813, 2011.

606 Hayes, D. J., Kicklighter, D. W., McGuire, A. D., Chen, M., Zhuang, Q., Yuan, F., Melillo, J. M., and

607 Wullschleger, S. D.: The impacts of recent permafrost thaw on land–atmosphere greenhouse gas

608 exchange, Environmental Research Letters, 9, 045005, 10.1088/1748-9326/9/4/045005, 2014.

609 Xiaolan He, Kate S. He, Jaakko Hyvönen, Will bryophytes survive in a warming world?,

610 Perspectives in Plant Ecology, Evolution and Systematics, Volume 19, 2016, Pages 49-60,

611 ISSN 1433-8319, https://doi.org/10.1016/j.ppees.2016.02.005.

612 Hiller, R. V., McFadden, J. P., and Kljun, N.: Interpreting CO2 Fluxes Over a Suburban Lawn: The

613 Influence of Traffic Emissions, Boundary-Layer Meteorology, 138, 215-230, 10.1007/s10546-010-9558-

614 0, 2010.

615 Hugelius, G., Strauss, J., Zubrzycki, S., Harden, J. W., Schuur, E. A. G., Ping, C. L., Schirrmeister, L.,

616 Grosse, G., Michaelson, G. J., Koven, C. D., amp, apos, Donnell, J. A., Elberling, B., Mishra, U., Camill,

617 P., Yu, Z., Palmtag, J., and Kuhry, P.: Estimated stocks of circumpolar permafrost carbon with quantified

618 uncertainty ranges and identified data gaps, Biogeosciences, 11, 6573-6593, 10.5194/bg-11-6573-2014,

619 2014.

620 Jägerbrand, A. K., Lindblad, K. E. M., Björk, R. G., Alatalo, J. M., and Molau, U.: Bryophyte and Lichen

621 Diversity Under Simulated Environmental Change Compared with Observed Variation in Unmanipulated

622 Alpine Tundra, Biodiversity and Conservation, 15, 4453-4475, 10.1007/s10531-005-5098-1, 2006.

623 Jenkins, J. P., Richardson, A. D., Braswell, B. H., Ollinger, S. V., Hollinger, D. Y., and Smith, M. L.:

624 Refining light-use efficiency calculations for a deciduous forest canopy using simultaneous tower-based

625 carbon flux and radiometric measurements, Agricultural and Forest Meteorology, 143, 64-79,

626 10.1016/j.agrformet.2006.11.008, 2007.

627 Juha M Alatalo, Annika K Jägerbrand, Mohammad Bagher Erfanian, Shengbin Chen, Shou-Qin Sun, Ulf

628 Molau, Bryophyte cover and richness decline after 18 years of experimental warming in alpine Sweden,

629 AoB PLANTS, Volume 12, Issue 6, December 2020, plaa061, https://doi.org/10.1093/aobpla/plaa061

Kasischke, E. S.: Boreal ecosystems in the global carbon cycle. In Fire, climate change, and carbon cycling in the boreal forest, Ecological Studies (Analysis and Synthesis), 138, 19-30, https://doi.org/10.1007/978-0-387-21629-4_2, 2000.

Kasischke, E. S., and Turetsky, M. R.: Recent changes in the fire regime across the North American boreal region—Spatial and temporal patterns of burning across Canada and Alaska, Geophysical Research Letters, 33, 10.1029/2006gl025677, 2006.

Kip, N., Ouyang, W., van Winden, J., Raghoebarsing, A., van Niftrik, L., Pol, A., Pan, Y., Bodrossy, L., van Donselaar, E. G., Reichart, G. J., Jetten, M. S., Damste, J. S., and Op den Camp, H. J.: Detection, isolation, and characterization of acidophilic methanotrophs from Sphagnum mosses, Applied and environmental microbiology, 77, 5643-5654, 10.1128/AEM.05017-11, 2011.

Knorr, W.: Annual and interannual CO2 exchanges of the terrestrial biosphere: process-based simulations and uncertainties, Global Ecology and Biogeography, 9, 225-252, 2000.

Koven, C. D., Schuur, E. A. G., Schädel, C., Bohn, T. J., Burke, E. J., Chen, G., Chen, X., Ciais, P., Grosse, G., Harden, J. W., Hayes, D. J., Hugelius, G., Jafarov, E. E., Krinner, G., Kuhry, P., Lawrence, D. M., Macdougall, A. H., Marchenko, S. S., Mcguire, A. D., Natali, S. M., Nicolsky, D. J., Olefeldt, D., Peng, S., Romanovsky, V. E., Schaefer, K. M., Strauss, J., Treat, C. C. & Turetsky, M. 2015. A simplified, data-constrained approach to estimate the permafrost carbon-climate feedback. *Philosophical Transactions of the Royal Society A: Mathematical, Physical and Engineering Sciences,* 373.

L. Kulmala, J. P., P. Hari and T. Vesala: Photosynthesis of ground vegetation in different aged pine forests: Effect of environmental factors predicted with a process-based model, Journal of Vegetation Science, 22, 96–110, 2011.

Launiainen, S., Katul, G. G., Lauren, A., and Kolari, P.: Coupling boreal forest CO2, H2O and energy flows by a vertically structured forest canopy – Soil model with separate bryophyte layer, Ecological Modelling, 312, 385-405, 10.1016/j.ecolmodel.2015.06.007, 2015.

Lindo, Z., and Gonzalez, A.: The Bryosphere: An Integral and Influential Component of the Earth's Biosphere, Ecosystems, 13, 612-627, 10.1007/s10021-010-9336-3, 2010.

Lang, S.I., Cornelissen, J.H.C., Shaver, G.R., Ahrens, M., Callaghan, T.V., Molau, U., Ter Braak, C.J.F., Hölzer, A. and Aerts, R. (2012), Arctic warming on two continents has consistent negative effects on lichen diversity and mixed effects on bryophyte diversity. Glob Change Biol, 18: 1096-1107. https://doi.org/10.1111/j.1365-2486.2011.02570.x

Longton, R. E.: Adaptations and strategies of polar bryophytes, Botanical Journal of the Linnean Society, 98, 253-268, 1988.

Markham, J. H.: Variation in moss-associated nitrogen fixation in boreal forest stands, Oecologia, 161, 353-359, 10.1007/s00442-009-1391-0, 2009.

664 McEwing, K. R., Fisher, J. P., and Zona, D.: Environmental and vegetation controls on the spatial

665 variability of CH4 emission from wet-sedge and tussock tundra ecosystems in the Arctic, Plant and soil,

666 388, 37-52, 10.1007/s11104-014-2377-1, 2015.

667 McGuire, A. D., Melillo, J. M., Joyce, L. A., Kicklighter, D. W., Grace, A. L., III, B. M., and Vorosmarty,

668 C. J.: Interactions between carbon and nitrogen dynamics in estimating net primary productivity for

669 potential vegetation in North America, Global Biogeochemical Cycles, 6, 101-124, 1992.

670 McGuire, A. D., Melillo, J. M., Kicklighter, D. W., and Joyce, L. A.: Equilibrium responses of soil carbon

671 to climate change: Empirical and process-based estimates, Journal of Biogeography, 785-796, 1995.

672 McGuire, A. D., and Hobbie, J. E.: Global climate change and the equilibrium responses of carbon

673 storage in arctic and subarctic regions, In Modeling the Arctic system: A workshop report on the state of

674 modeling in the Arctic System Science program, 53-54, 1997.

675 McGuire, A. D., Anderson, L. G., Christensen, T. R., Dallimore, S., Guo, L., Hayes, D. J., Heimann, M.,

676 Lorenson, T. D., Macdonald, R. W., and Roulet, N.: Sensitivity of the carbon cycle in the Arctic to climate

677 change, Ecological Monographs, 79, 523-555, 2009.

678 Melillo, J. M., McGuire, A. D., Kicklighter, D. W., Moore, B., Vorosmarty, C. J., and Schloss, A. L.:

679 Global climate change and terrestrial net primary production, Nature, 363, 234, 10.1038/363234a0, 1993.

680 Melillo, J. M., Butler, S., Johnson, J., Mohan, J., Steudler, P., Lux, H., Burrows, E., Bowles, F., Smith, R.,

681 Scott, L., Vario, C., Hill, T., Burton, A., Zhou, Y.-M., and Tang, J.: Soil warming, carbon - nitrogen

682 interactions, and forest carbon budgets, PNAS, 108, 9508-9512, 2011.

683 Naomi Oreskes, K. S.-F., Kenneth Belitz: Verification, validation, and confirmation of numerical models

684 in the earth sciences, Science, 263, 641-646, 1994.

685 O. Skre, W. C. O.: Moss production in a black spruce Picea mariana forest with permafrost near

686 Fairbanks, Alaska, as compared with two permafrost-free stands, Ecography, 2, 249-254, 1979.

687 Oechel, W. C., Laskowski, C. A., Burba, G., Gioli, B., and Kalhori, A. A. M.: Annual patterns and budget

688 of CO2flux in an Arctic tussock tundra ecosystem, Journal of Geophysical Research: Biogeosciences,

689 119, 323-339, 10.1002/2013jg002431, 2014.

690 Okland, R. H.: Population Biology of the Clonal Moss Hylocomium Splendens in Norwegian Boreal

691 SpruceForests. I. Demography, Journal of Ecology, 83, 697-712, 1995.

692 P.C. Harley, J. D. T., K.J. Murray, and J. Beyers: Irradiance and temperature effects on photosynthesis of

693 tussock tundra Sphagnum mosses from the foothills of the Philip Smith Mountains, Alaska, Oecologia,

694 79, 251-259, 1989.

695 Pakarinen, P., and D. H. Vitt: Primary production of plant communities of the Truelove Lowland, Devon

696 Island, Canada–Moss communities, Primary production and production processes, tundra biome.

697 International Biological Programme, Tundra Biome Steering Committee, Edmonton Oslo, 37-46, 1973.

698 Pharo, E. J., and Zartman, C. E.: Bryophytes in a changing landscape: The hierarchical effects of habitat

699 fragmentation on ecological and evolutionary processes, Biological Conservation, 135, 315-325,

700 10.1016/j.biocon.2006.10.016, 2007.

701 Raich, J. W., Rastetter, E. B., Melillo, J. M., Kicklighter, D. W., Steudler, P. A., Peterson, B. J., Grace, A.

702 L., III, B. M., and Vorosmarty, C. J.: Potential net primary productivity in South America: application of a

703 global model, Ecological Applications, 1, 399-429, 1991.

704 Richardson, A. D., Jenkins, J. P., Braswell, B. H., Hollinger, D. Y., Ollinger, S. V., and Smith, M. L.: Use

705 of digital webcam images to track spring green-up in a deciduous broadleaf forest, Oecologia, 152, 323-

706 334, 10.1007/s00442-006-0657-z, 2007.

707 Running, S. W., and Coughlan, J. C.: A general model of forest ecosystem processes for regional

708 applications I. Hydrologic balance, canopy gas exchange and primary production processes., Ecological

709 Modelling, 42, 125-154, 1988.

710 S. Frolking, M. L. G., S.C. Wofsy, S-M. Fan, D.J. Sutton, J.W. Munger, A.M. Bazzaz, B.C. Daube, P.M.

711 Crill, J.D, Aber, L.E. Band, X. Wang, K. Savage, T. Moore and R.C. Harriss: Modelling temporal

712 variability in the carbon balance of a spruce/moss boreal forest, Global change biology, 2, 343-366, 1996.

713 Sarah E. Hobbie, J. P. S., Susan E. Trumore and James R. Randerson: Controls over carbon storage and

714 turnover in high-latitude soils, Global change biology, 6, 196-210, 2000.

715 Schimel, D. S., House, J. I., Hibbard, K. A., Bousquet, P., Ciais, P., Peylin, P., Braswell, B. H., Apps, M.

716 J., Baker, D., Bondeau, A., Canadell, J., Churkina, G., Cramer, W., Denning, A. S., Field, C. B.,

717 Friedlingstein, P., Goodale, C., Heimann, M., Houghton, R. A., Melillo, J. M., III, B. M., Murdiyarso, D.,

718 Noble, I., Pacala, S. W., Prentice, I. C., Raupach, M. R., Rayner, P. J., Scholes, R. J., Steffen, W. L., and

719 Wirth, C.: Recent patterns and mechanisms of carbon exchange by terrestrial ecosystems, Nature, 414,

720 2001.

721 Serreze, M. C., and Francis, J. A.: The Arctic on the fast track of change, Weather, 61, 65-69, 2006.

722 Shetler, G., Turetsky, M. R., Kane, E., and Kasischke, E.: Sphagnum mosses limit total carbon

723 consumption during fire in Alaskan black spruce forests, Canadian Journal of Forest Research, 38, 2328-

724 2336, 10.1139/x08-057, 2008.

725 Soja, A. J., Tchebakova, N. M., French, N. H. F., Flannigan, M. D., Shugart, H. H., Stocks, B. J.,

726 Sukhinin, A. I., Parfenova, E. I., Chapin, F. S., and Stackhouse, P. W.: Climate-induced boreal forest

727 change: Predictions versus current observations, Global and Planetary Change, 56, 274-296,

728 10.1016/j.gloplacha.2006.07.028, 2007.

729 Stow, D. A., Hope, A., McGuire, D., Verbyla, D., Gamon, J., Huemmrich, F., Houston, S., Racine, C.,

730 Sturm, M., Tape, K., Hinzman, L., Yoshikawa, K., Tweedie, C., Noyle, B., Silapaswan, C., Douglas, D.,

731 Griffith, B., Jia, G., Epstein, H., Walker, D., Daeschner, S., Petersen, A., Zhou, L., and Myneni, R.:

732 Remote sensing of vegetation and land-cover change in Arctic Tundra Ecosystems, Remote Sensing of

733 Environment, 89, 281-308, 10.1016/j.rse.2003.10.018, 2004.

734 T. G. Williams, L. B. F.: Measuring and modelling environmental influences on photosynthetic gas

735 exchange in Sphagnum and Pleurozium, Plant, Cell and Environment, 21, 555–564, 1998.

736 Tang, J., and Zhuang, Q.: Equifinality in parameterization of process-based biogeochemistry models: A

737 significant uncertainty source to the estimation of regional carbon dynamics, Journal of Geophysical

738 Research: Biogeosciences, 113, 10.1029/2008jg000757, 2008.

739 Tape, K. E. N., Sturm, M., and Racine, C.: The evidence for shrub expansion in Northern Alaska and the

740 Pan-Arctic, Global change biology, 12, 686-702, 10.1111/j.1365-2486.2006.01128.x, 2006.

741 Tarnocai, C., Canadell, J. G., Schuur, E. A. G., Kuhry, P., Mazhitova, G., and Zimov, S.: Soil organic

742 carbon pools in the northern circumpolar permafrost region, Global Biogeochemical Cycles, 23, n/a-n/a,

743 10.1029/2008gb003327, 2009.

744 Todd-Brown, K. E. O., Randerson, J. T., Post, W. M., Hoffman, F. M., Tarnocai, C., Schuur, E. A. G., and

745 Allison, S. D.: Causes of variation in soil carbon simulations from CMIP5 Earth system models and

746 comparison with observations, Biogeosciences, 10, 1717-1736, 10.5194/bg-10-1717-2013, 2013.

747 Treseder, K. K., Balser, T. C., Bradford, M. A., Brodie, E. L., Dubinsky, E. A., Eviner, V. T., Hofmockel,

748 K. S., Lennon, J. T., Levine, U. Y., MacGregor, B. J., Pett-Ridge, J., and Waldrop, M. P.: Integrating

749 microbial ecology into ecosystem models: challenges and priorities, Biogeochemistry, 109, 7-18,

750 10.1007/s10533-011-9636-5, 2011.

751 Treseder, K. K., Marusenko, Y., Romero-Olivares, A. L., and Maltz, M. R.: Experimental warming alters

752 potential function of the fungal community in boreal forest, Global change biology, 22, 3395-3404,

753 10.1111/gcb.13238, 2016.

754 Turetsky, M. R., Mack, M. C., Hollingsworth, T. N., and Harden, J. W.: The role of mosses in ecosystem

755 succession and function in Alaska's boreal forest, Canadian Journal of Forest Research, 40, 1237-1264,

756 10.1139/x10-072, 2010.

757 Turetsky, M. R., Bond-Lamberty, B., Euskirchen, E., Talbot, J., Frolking, S., McGuire, A. D., and Tuittila,

758 E. S.: The resilience and functional role of moss in boreal and arctic ecosystems, The New phytologist,

759 196, 49-67, 10.1111/j.1469-8137.2012.04254.x, 2012.

760 Wardle, M.-C. N. a. D. A.: Understory vegetation as a forest ecosystem driver: evidence from the northern

761 Swedish boreal forest, The Ecological Society of America, 3, 421–428, 2005.

762 White, A., Cannell, M. G. R., and Friend, A. D.: The high-latitude terrestrial carbon sink: a model analysis

763 Global change biology, 6, 227-245, 2000.

764 Wieder, W. R., Bonan, G. B., and Allison, S. D.: Global soil carbon projections are improved by

765 modelling microbial processes, Nature Climate Change, 3, 909-912, 10.1038/nclimate1951, 2013.

766   Zha, J., and Zhuang, Q.: Microbial decomposition processes and vulnerable Arctic soil organic carbon in

767   the 21st century, Biogeosciences Discussions, 1-34, 10.5194/bg-2018-241, 2018.

768   Zhuang, Q., Romanovsky, V. E., and McGuire, A. D.: Incorporation of a permafrost model into a large-

769   scale ecosystem model: Evaluation of temporal and spatial scaling issues in simulating soil thermal

770   dynamics, Journal of Geophysical Research: Atmospheres, 106, 33649-33670, 10.1029/2001jd900151,

771   2001.

772   Zhuang, Q., McGuire, A. D., O'Neill, K. P., Harden, J. W., Romanovsky, V. E., and Yarie, J.: Modeling

773   soil thermal and carbon dynamics of a fire chronosequence in interior Alaska, Journal of Geophysical

774   Research, 108, 10.1029/2001jd001244, 2002.

775   Zhuang, Q., A. D. McGuire, J. M. Melillo, J. S. Clein, R. J. Dargaville, D. W. Kicklighter, R. B. Myneni,

776   J. Dong, V. E. Romanovsky, J. Harden, J. E. Hobbie (2003) Carbon cycling in extratropical terrestrial

777   ecosystems of the Northern Hemisphere during the 20th Century: A modeling analysis of the influences of

778   soil thermal dynamics, Tellus, 55B, 751-776, 2003

779   Zhuang, Q., He, J., Lu, Y., Ji, L., Xiao, J., and Luo, T.: Carbon dynamics of terrestrial ecosystems on the

780   Tibetan Plateau during the 20th century: an analysis with a process-based biogeochemical model, Global

781   Ecology and Biogeography, 19, 649-662, 10.1111/j.1466-8238.2010.00559.x, 2010.

782   Zhuang, Q., Chen, M., Xu, K., Tang, J., Saikawa, E., Lu, Y., Melillo, J. M., Prinn, R. G., and McGuire, A.

783   D.: Response of global soil consumption of atmospheric methane to changes in atmospheric climate and

784   nitrogen deposition, Global Biogeochemical Cycles, 27, 650-663, 10.1002/gbc.20057, 2013.

785   Zhuang, Q., Zhu, X., He, Y., Prigent, C., Melillo, J. M., David McGuire, A., Prinn, R. G., and Kicklighter,

786   D. W.: Influence of changes in wetland inundation extent on net fluxes of carbon dioxide and methane in

787   northern high latitudes from 1993 to 2004, Environmental Research Letters, 10, 095009, 10.1088/1748-

788   9326/10/9/095009, 2015.

789

790

791

792

793

794

795

796   **Author contributions.** Q.Z. designed the study. J.Z. conducted model development, simulation

797   and analysis. J.Z. and Q. Z. wrote the paper.

798   **Competing financial interests.** The submission has no competing financial interests.

799   **Materials & Correspondence.** Correspondence and material requests should be addressed to

800   qzhuang@purdue.edu.

801

802

803

804

805

806

807

808

809

810

811
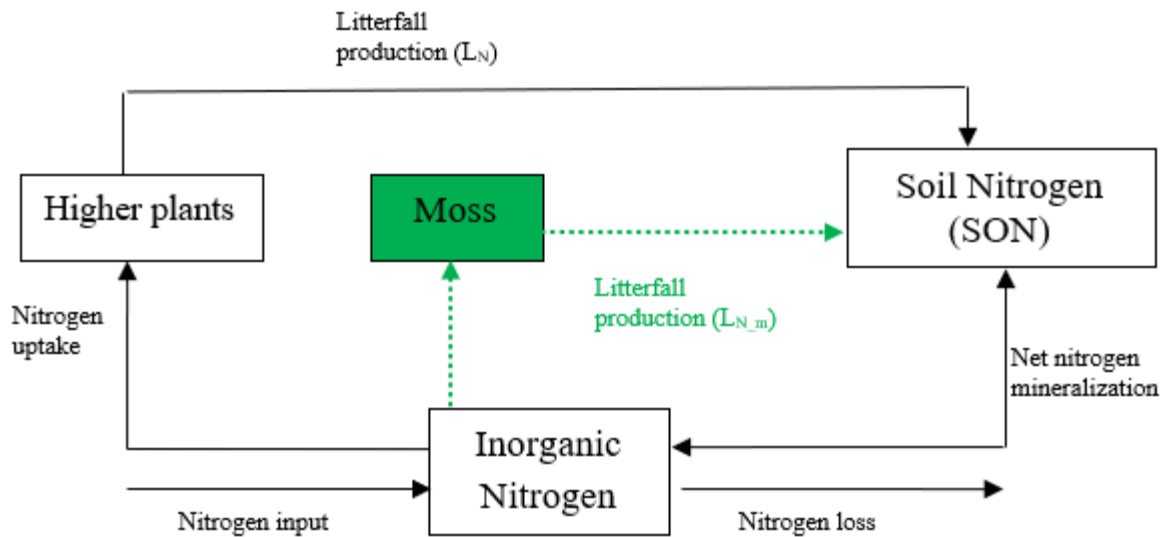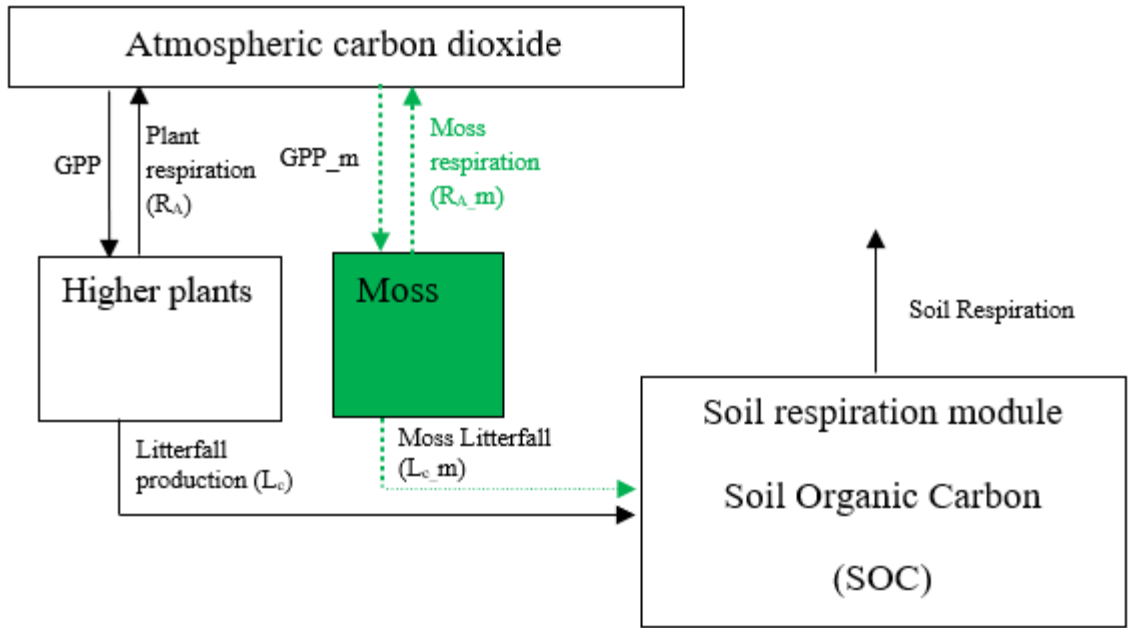
Figure 1. Schematic diagram of TEM_Moss: Green dashed arrows are new carbon and nitrogen
fluxes, representing moss production, moss respiration and litterfall of moss. Black arrows were
in TEM 5.0 (Zhuang et al., 2013).

815

816
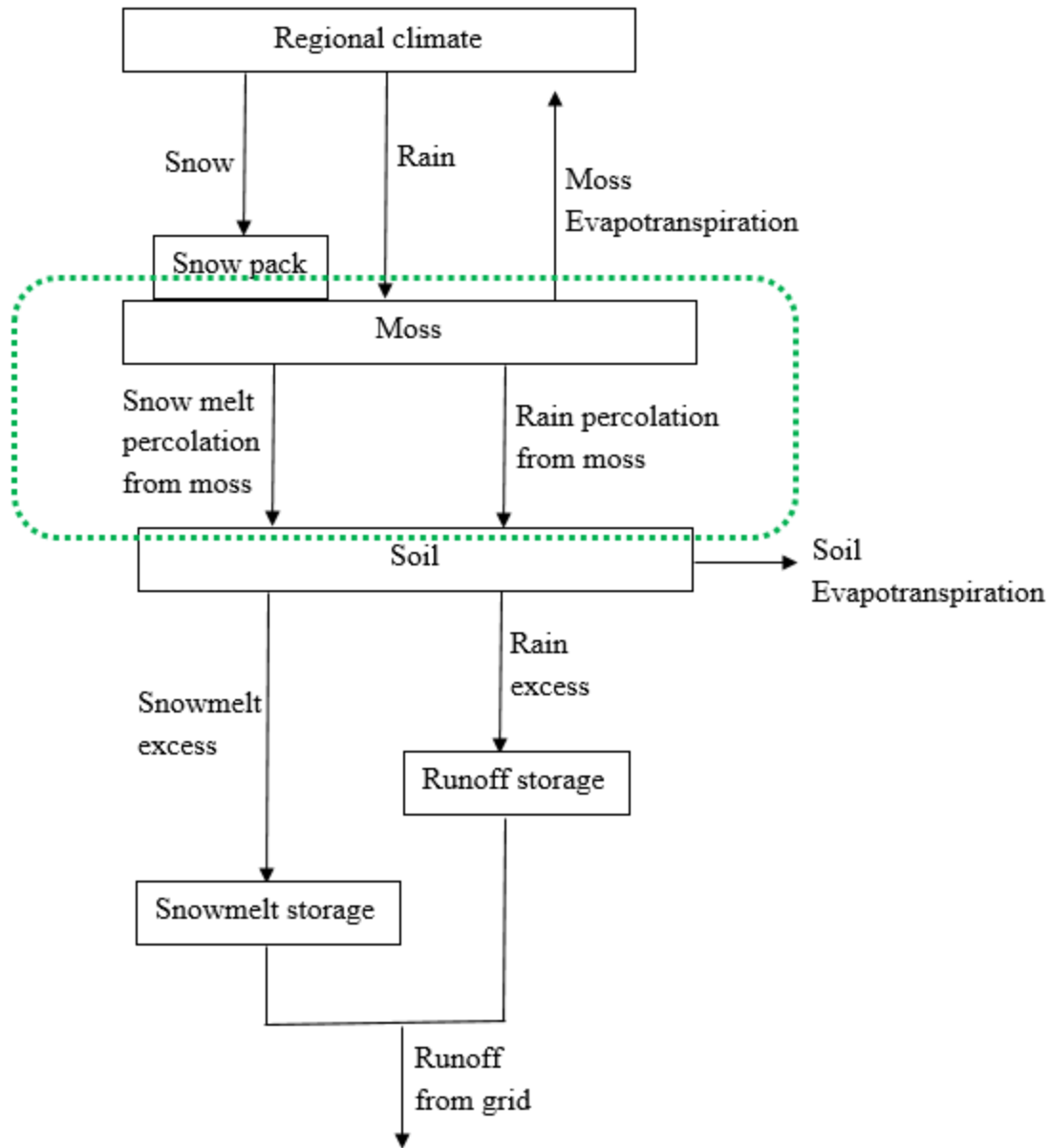
817

818   Figure 2. The revised Water Balance Model: Green dashed circle represents the hydrology
819   dynamics for moss (Vörösmarty et al., 1989).

820

821

822

823

824

825
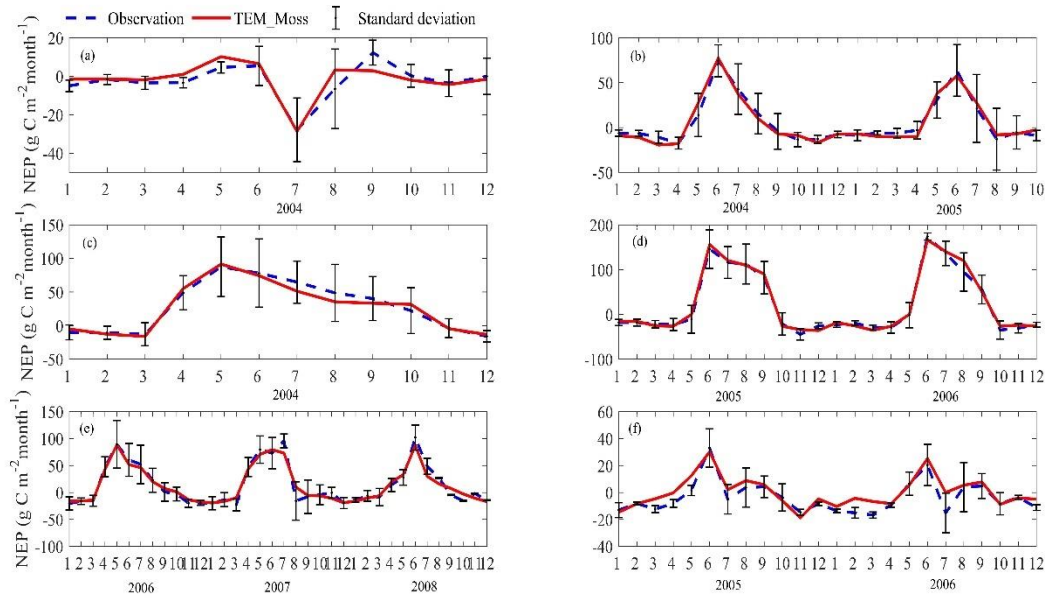
Figure 3. Comparison between observed and simulated NEP (g C m^{-2}month^{-1}) at: (a) Ivotuk
(alpine tundra), (b) UCI-1964 burn site (boreal forest), (c) Howland Forest (temperate coniferous
forest), (d) Univ. of Mich. Biological Station (Temperate deciduous forest), (e) KUOM Turfgrass
Field (Grassland), and (f) Atqasuk (Wet tundra). Error bars represent standard errors among
daily in one month.

831

832

833

834

835

836

837
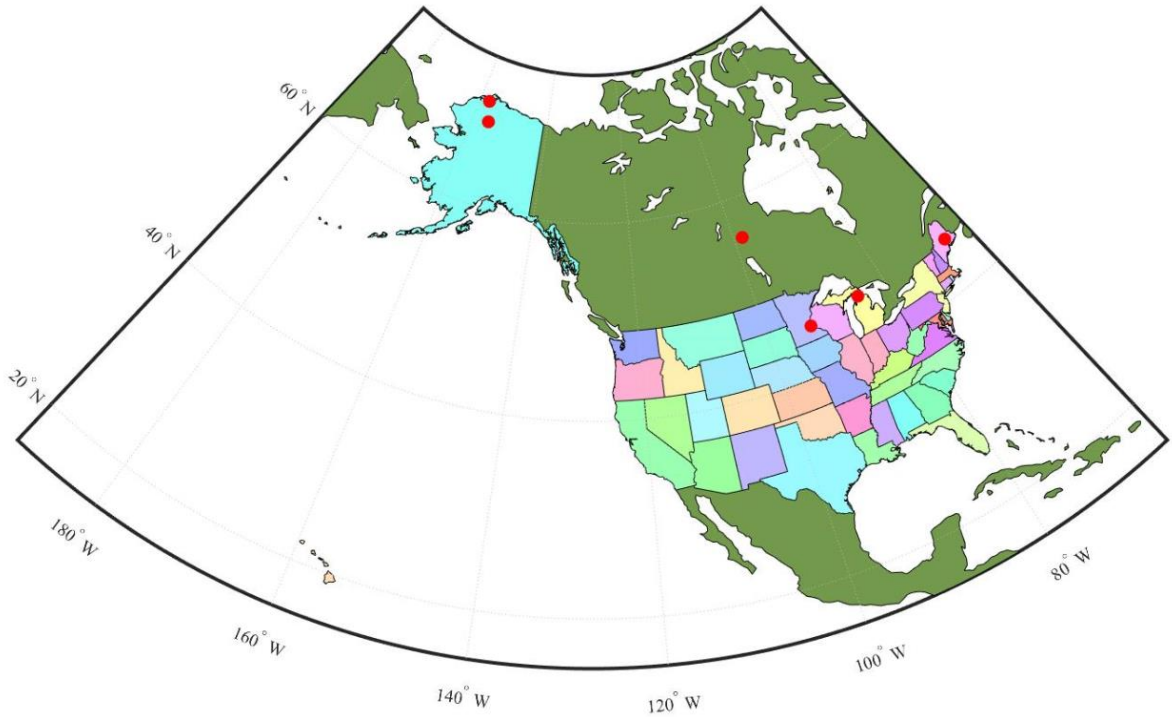
Figure 4. Map showing six sites used for TEM_Moss calibration. The red points represent the six
sites, five are in the US and one is in the Canada: US-Ivo: Ivotuk (alpine tundra), CA-NS3: UCI-
1964 burn site (boreal forest), US-Ho1: Howland Forest (temperate coniferous forest), US-UMB:
Univ. of Mich. Biological Station (temperate deciduous forest), US-KUT: KUOM Turfgrass
Field (grassland), US-Atq: Atqasuk (wet tundra).

843

844

845

846

847

848

849

850

851

852

853

854

855
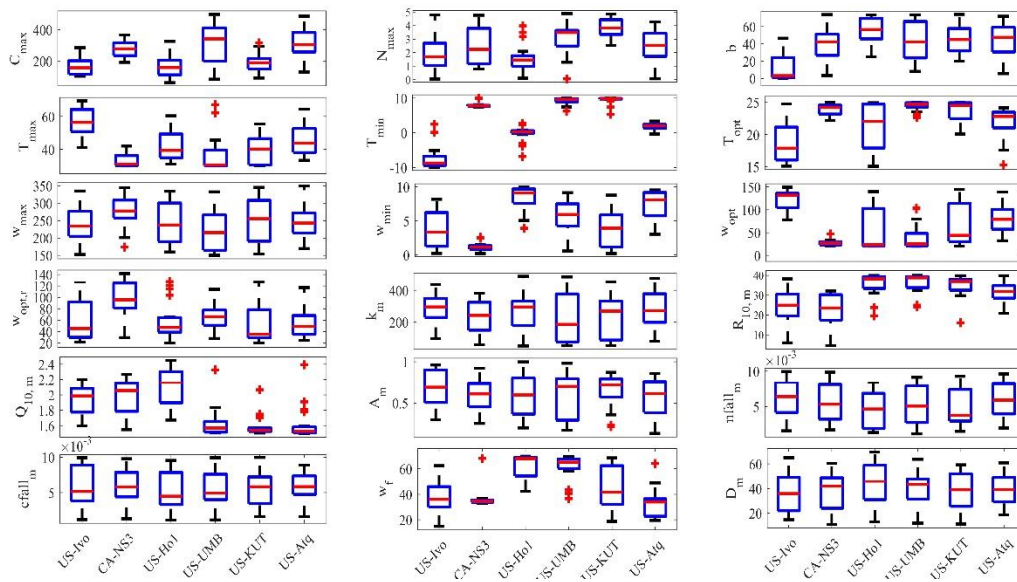
Figure 5. Boxplot of parameter posterior distribution that are obtained after ensemble inverse modeling for TEM_Moss at all six sites: US-Ivo: Ivotuk (alpine tundra), CA-NS3: UCI-1964 burn site (boreal forest), US-Ho1: Howland Forest (temperate coniferous forest), US-UMB: Univ. of Mich. Biological Station (temperate deciduous forest), US-KUT: KUOM Turfgrass Field (grassland), US-Atq: Atqasuk (wet tundra). Boxes represent the range between the first quartile and the third quartile of the parameter values, the red line within box represents the second quartile or the mean of the values. The bottom and top whiskers represent minimum and maximum parameter values, respectively.

856
857
858
859
860
861
862
863
864
865
866
867
868
869

870

871
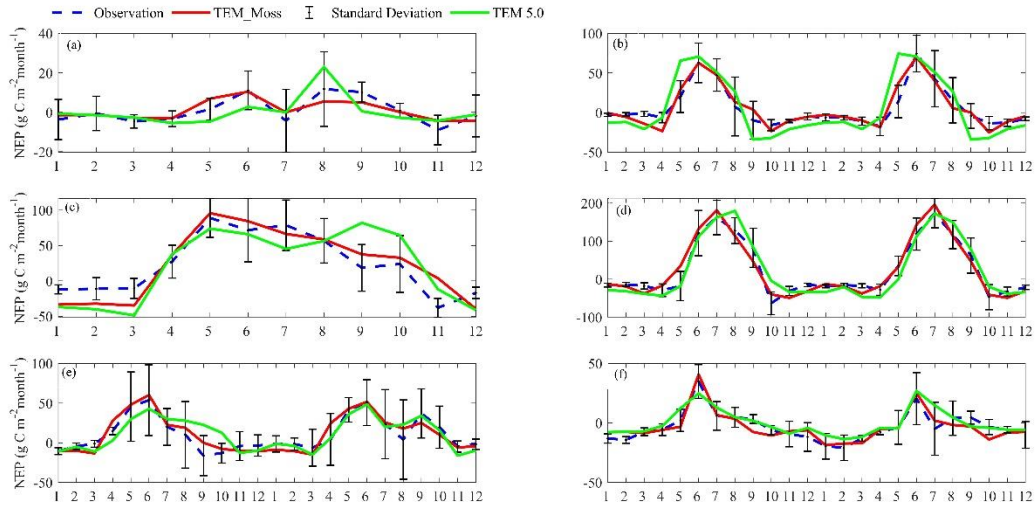
Figure 6. Comparison between observed and simulated NEP (g C m^{-2}month^{-1}) at: (a) Ivotuk (alpine tundra), (b) UCI-1964 burn site (boreal forest), (c) Howland Forest (temperate coniferous forest), (d) Bartlett Experimental Forest (Temperate deciduous forest), (e) Brookings (Grassland), and (f) Atqasuk (Wet tundra).

876

877

878

879

880

881

882

883

884

885

886

887

888
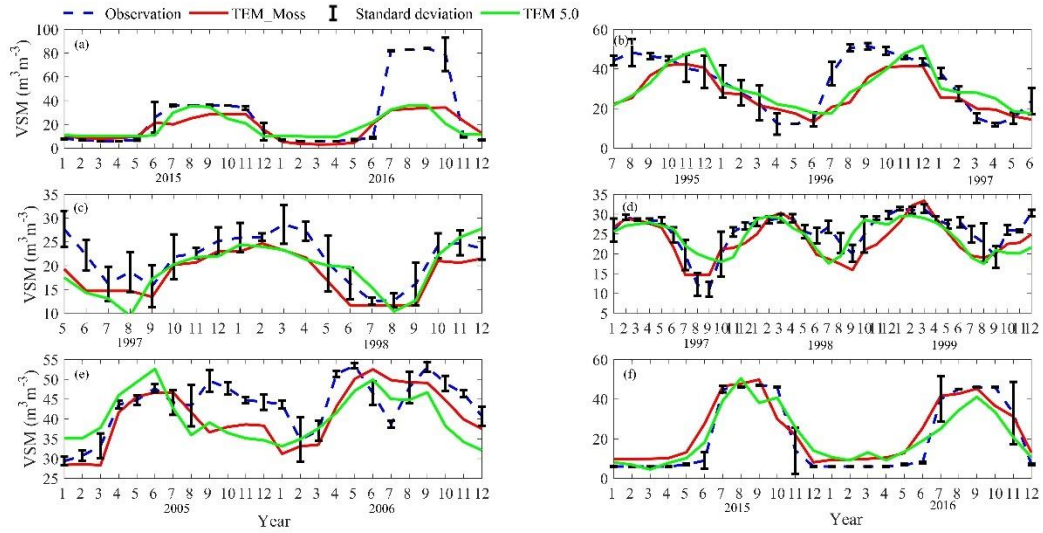
Figure 7. Comparison between observed and simulated volumetric soil moisture (VSM, m^3m^{-3}) at: (a) US-Ivo (alpine tundra), (b) BOREAS NSA-OBS (boreal forest), (c) NL-Loo (temperate coniferous forest), (d) DK-Sor (Temperate deciduous forest), (e) US-Bkg (Grassland), and (f) US-Atq (Wet tundra).

889

890

891

892

893

894

895

896

897

898

899

900

901

902

903
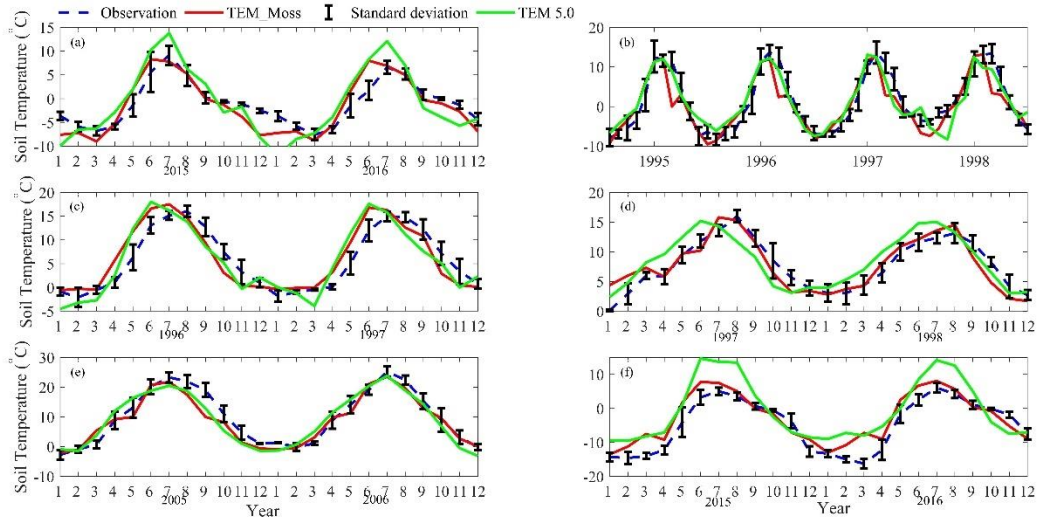
904

905 Figure 8. Comparison between observed and simulated soil temperature at 5cm depth (℃) at: (a)
906 US-Ivo (alpine tundra), (b) BOREAS NSA-OBS (boreal forest), (c) US-Ho1 (temperate
907 coniferous forest), (d) BE-Vie (Temperate deciduous forest), (e) US-Bkg (Grassland), and (f)
908 US-Atq (Wet tundra).

909

910

911

912

913

914

915

916

917

918

919

920

921

922
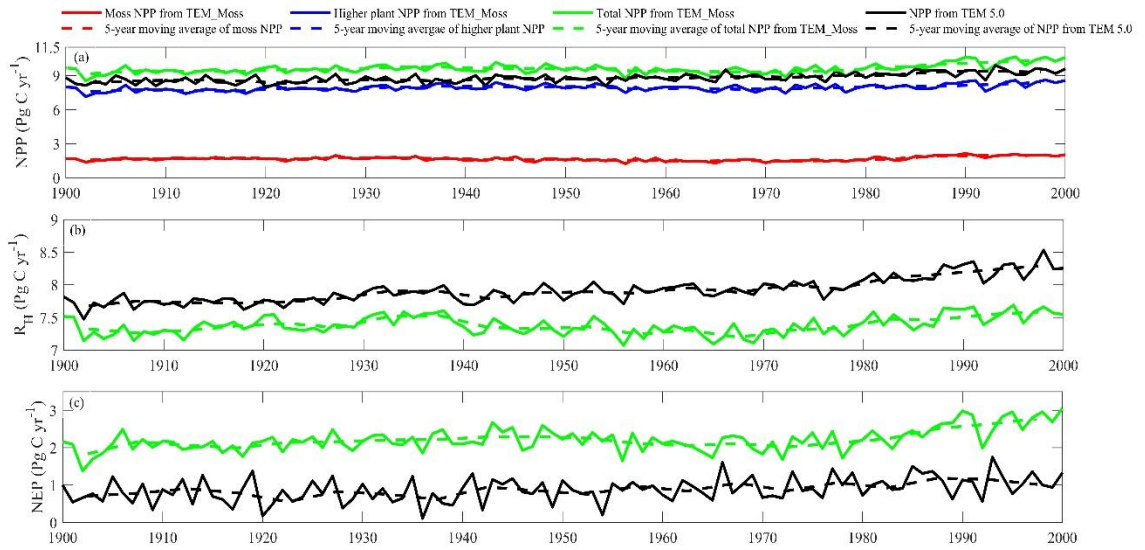
Figure 9. Simulated annual net primary production (NPP, a), heterotrophic respiration (R_H, b), and net ecosystem production (NEP, c) during the 20th century by TEM_Moss and TEM 5.0.

923
924

925

926

927

928

929

930

931

932

933

934

935

936

937

938

939

940
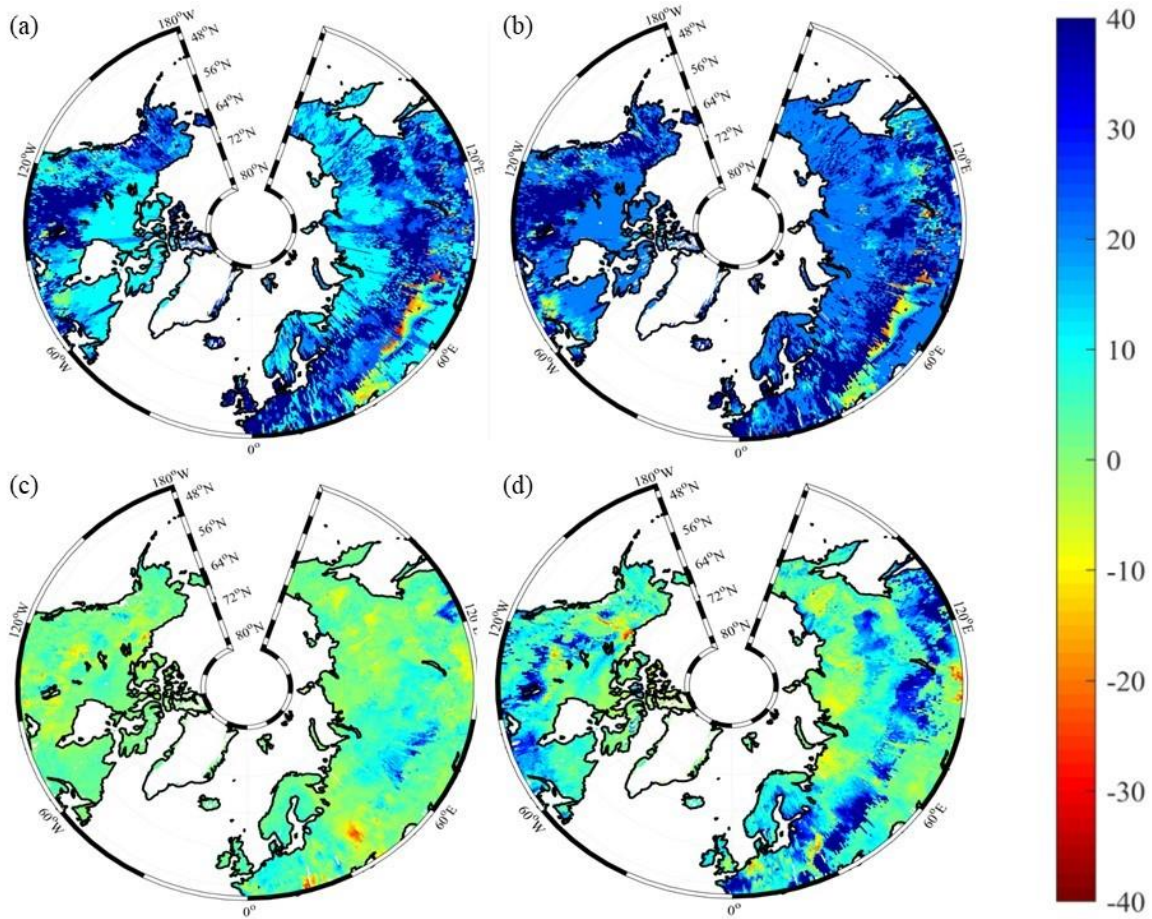
941

942   Figure 10. Spatial distribution of NEP simulated by TEM_Moss for the periods (a) 1900–1950,
943   (b) 1951–2000, and by TEM 5.0 for the periods (c) 1900–1950, (d) 1951–2000. Positive values
944   of NEP represent sinks of CO_2 into terrestrial ecosystems, while negative values represent
945   sources of CO_2 to the atmosphere.

946

947

948

949

950

951

952

953

954

955
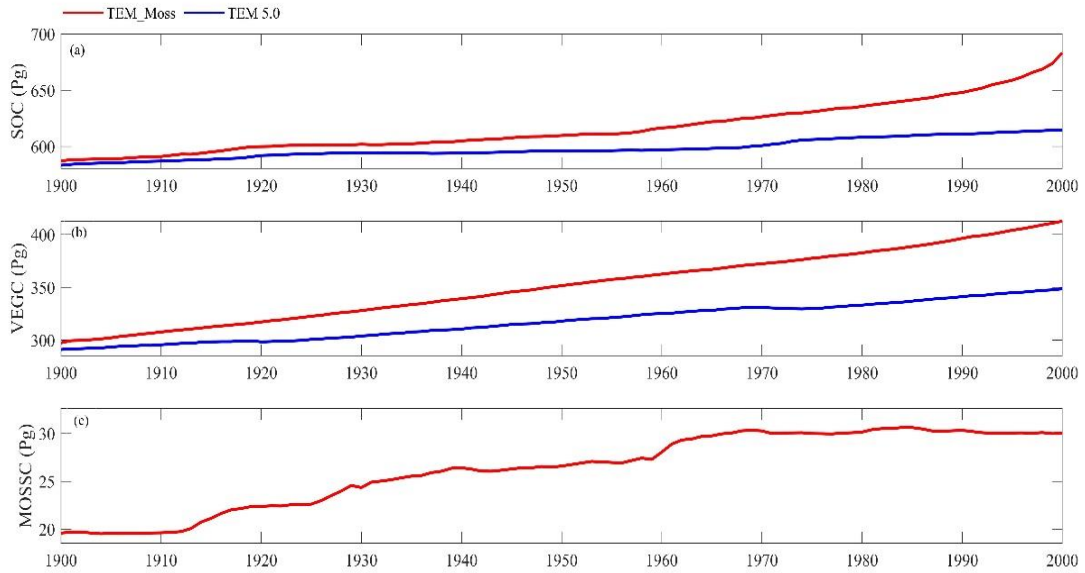
956

957 Figure 11. Simulated annual soil organic carbon (SOC, a), vegetation carbon (VEGC, b), and
958 moss carbon (MOSSC, c) during the 20th century by TEM_Moss and TEM 5.0.

959

960

961

962

963

964

965

966

967

968

969

970

971

972

973

974
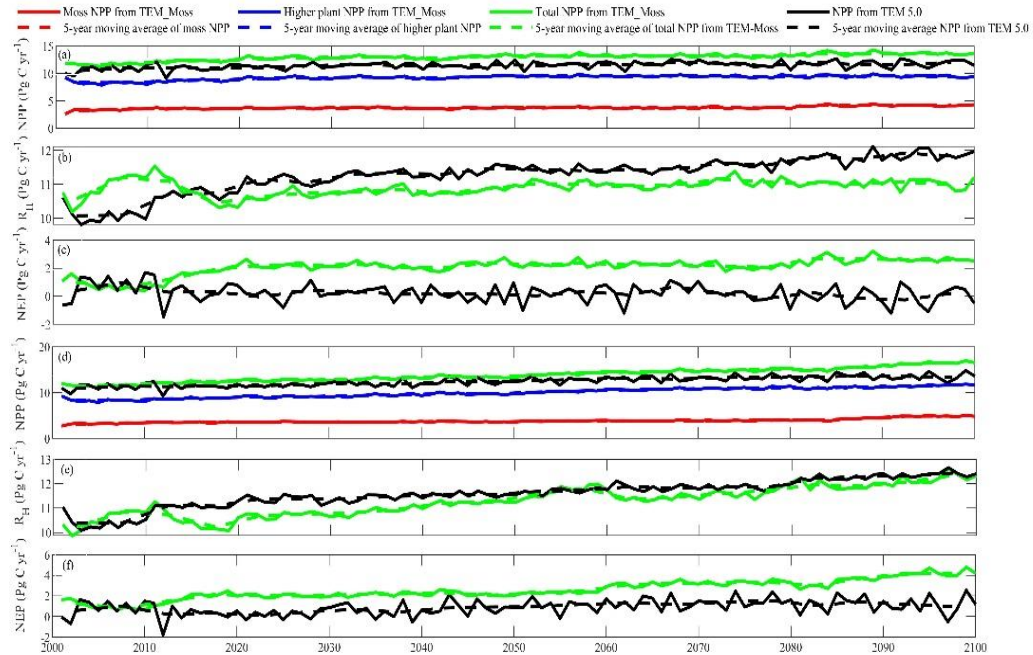
975

976 Figure 12. Predicted changes in carbon fluxes: annual net primary production (NPP, (a, d)),
977 heterotrophic respiration (R_H, (b, e)), and net ecosystem production (NEP, (c, f)) during the 21st
978 century under RCP 2.6 scenario (a, b, c) and RCP 8.5 scenario (d, e, f) by TEM_Moss and TEM
979 5.0.

980

981

982

983

984

985

986

987

988
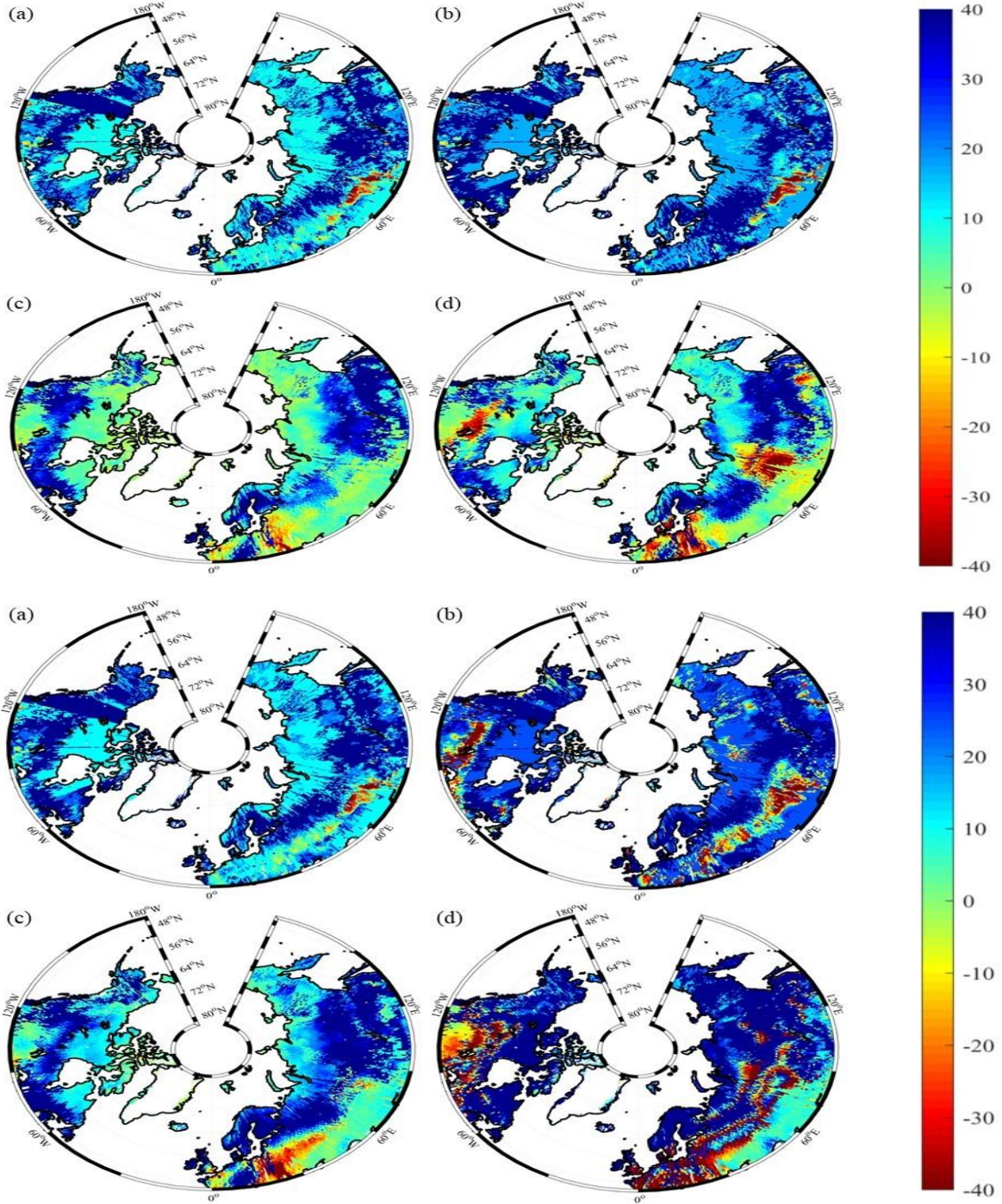
Figure 13. Spatial distribution of NEP simulated for the periods (a) 2000–2050, (b) 2051–2099
by TEM_Moss, and by TEM 5.0 (c, d) during the 21st century under RCP 2.6 scenario (upper
panel) and RCP 8.5 scenario (bottom panel). Positive values of NEP represent sinks of CO_2 into
terrestrial ecosystems, while negative values represent sources of CO_2 to the atmosphere.

993

994
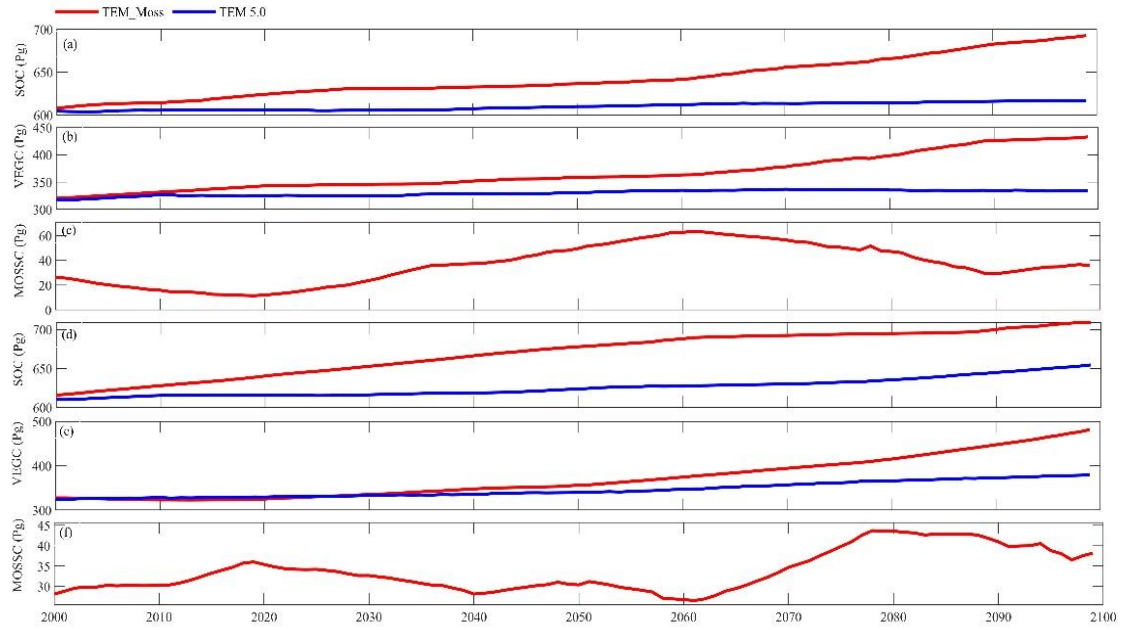
995

996 Figure 14. Simulated annual soil organic carbon (SOC, (a, d)), vegetation carbon (VEGC, (b, e)),

997 and moss carbon (MOSSC, (c, f)) during the 21st century by TEM_Moss and TEM 5.0 under

998 RCP 2.6 scenario (a, b, c) and RCP 8.5 scenario (d, e, f).

999

1000

1001

1002

1003

1004

1005

1006

1007

1008

1009

1010

1011

1012

1013

1014   (a)

1015
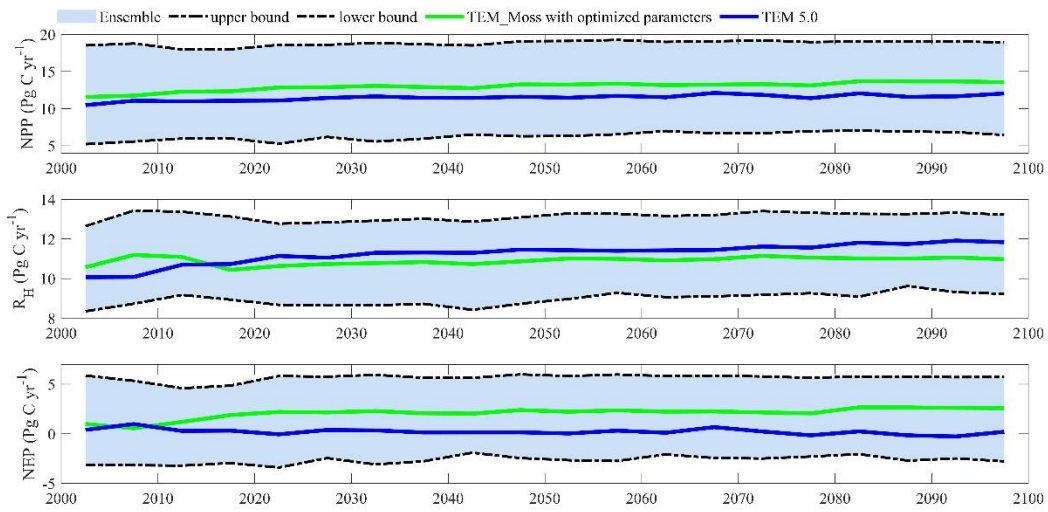
1016

1017   (b)

1018
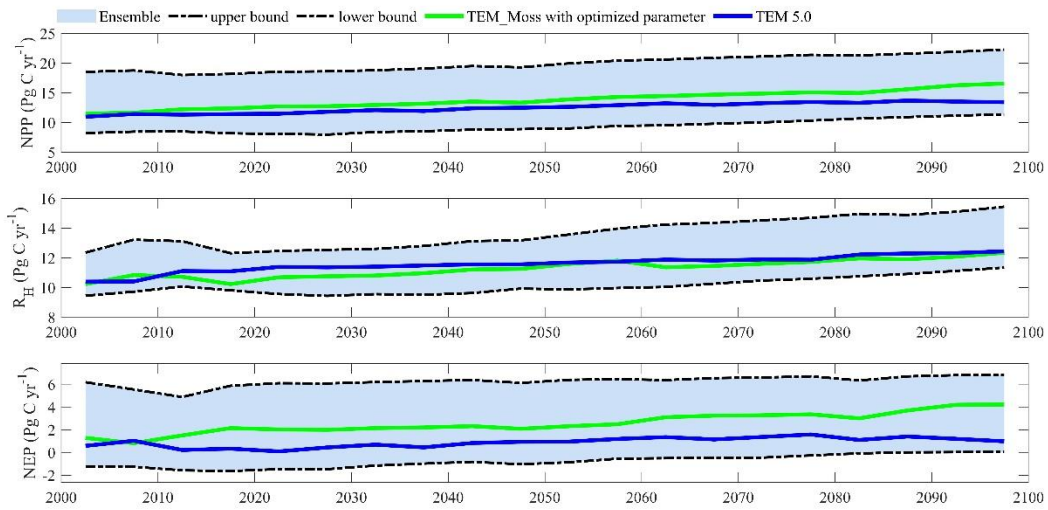
1019

1020   Figure 15. 5-year moving average plots for carbon fluxes under the (a) RCP 2.6 scenario and (b)
1021   RCP 8.5 scenario. The blue area represents the upper and lower bounds of simulations.

1022

1023

1024

 Table 1. Parameters associated with moss activities in TEM_Moss

Parameters	Units	descriptions	Parameter range (value)	references
C_{max}	$g\ C\ m^{-2}$	maximum rate of C assimilation	[50,500]	Launiainen et al. (2015); Williams &
b	$\mu mol\ m^{-2}$	Light half-saturation level	[5, 150]	Launiainen et al. (2015); Raich et al. (1991)
T_{min}	°C	minimum temperature	[-10, 10]	Frolking et al. (1996); Raich et al. (1991)
T_{max}	°C	maximum temperature	[30, 80]	Frolking et al. (1996); Raich et al. (1991)
T_{opt}	°C	optimal temperature	[15, 30]	Frolking et al. (1996); Raich et al. (1991)
w_{min}	mm	minimum water content for moss	[0.5, 15]	Frolking et al. (1996); Launiainen et al.
w_{max}	mm	maximum water content for moss	[150, 380]	Frolking et al. (1996); Launiainen et al. (2015)
w_{opt}	mm	optimal water content for moss	[10, 150]	Frolking et al. (1996); Zhuang et al. (2002)
k_m	$\mu L/L$	CO_2 concentration half-saturation level	[50, 500]	Zhuang et al. (2002); Raich et al. (1991)
$R_{10,\ m}$	$g\ C\ m^{-2}$	moss respiration rate at 10 °C	[0,40]	Frolking et al. (1996); Launiainen et al. (2015)
$Q_{10,\ m}$	$-$	moss respiration temperature sensitivity	[1.5, 2.5]	Frolking et al. (1996); Launiainen et al. (2015)
$w_{opt,\ r}$	mm	optimal water content for moss	[10, 150]	Frolking et al., 1996; Zhuang et al. (2002)
$cfall_m$	$g^{-1}g^{-1}\ mon^{-}$	constant proportion for carbon litterfall	[0.001, 0.01]	Zhuang et al. (2002); Raich et al. (1991)
N_{max}	$gN\ m^{-2}$	maximum rate of N uptake by mosses	[0.1,5]	Zhuang et al. (2002); Raich et al. (1991)
k_n	$g\ m^{-2}$	Half-saturation constant for N uptake by	1.0	Zhuang et al. (2002); Raich et al. (1991)
A_m	-	relative allocation of effort to C vs. N	[0,1]	Raich et al. (1991)
w_f	mm	moss field capacity	[10, 80]	Frolking et al. (1996); Raich et al. (1991)
$nfall_m$	$g^{-1}g^{-1}\ mon^{-}$	constant proportion for nitrogen litterfall	[0.001, 0.01]	Zhuang et al. (2002); Raich et al. (1991)
D_m	mm	Moss thickness	[0, 100]	Zhuang et al. (2002)

Table 2. Site description and measured NEP data used to calibrate TEM_Moss

Site Name	Location (Longitude (degrees) /Latitude (degrees))	Elevation (m)	Vegetation type	Description	Data range	Citations
Univ. of Mich. Biological Station	84.71W 45.56 N	234	Temperate deciduous forest	Located within a protected forest owned by the University of Michigan. Mean annual temperature is 5.83°C with mean annual precipitation of 803mm	01/2005- 12/2006	Gough et al. (2013)
Howland Forest (main tower)	68.74W 45.20N	60	Temperate coniferous forest	Closed coniferous forest, minimal disturbance.	01/2004- 12/2004	Davidson et al. (2006)
UCI-1964 burn site	98.38W 55.91N	260	Boreal forest	Located in a continental boreal forest, dominated by black spruce trees, within the BOREAS northern study area in central Manitoba, Canada.	01/2004- 10/2005	Goulden et al. (2006)
KUOM Turfgrass Field	93.19W 45.0N	301	Grassland	A low-maintenance lawn consisting of cool-season turfgrasses.	01/2006- 12/2008	Hiller et al. (2010)
Atqasuk	157.41W 70.47N	15	Wet tundra	100 km south of Barrow, Alaska. Variety of moist-wet coastal sedge tundra, and moist-tussock tundra surfaces in the more well-drained upland.	01/2005- 12/2006	Oechel et al. (2014);
Ivotuk	155.75W 68.49N	568	Alpine tundra	300 km south of Barrow and is located at the foothill of the Brooks Range and is classified as tussock sedge, dwarf-shrub, moss tundra.	01/2004- 12/2004	McEwing et al. (2015)

Table 3. Site description and measured NEP data used to validate TEM_Moss

Site Name	Location (Longitude (degrees) /Latitude (degrees))	Elevation (m)	Vegetation type	Description	Data range	Citations
Bartlett Experimental Forest	71.29W/ 44.06N	272	Temperate deciduous forest	Located within the White Mountains National Forest in north-central New Hampshire, USA, with mean annual temperature of 5.61 °C and mean annual precipitation of 1246mm.	01/2005- 12/2006	Jenkins et al. (2007); Richardson et al. (2007)
Howland Forest (main tower)	68.74W/ 45.20N	60	Temperate coniferous forest	Closed coniferous forest, minimal disturbance.	01/2003- 12/2003	Davidson et al. (2006)
UCI-1964 burn site	98.38W/ 55.91N	260	Boreal forest	Located in a continental boreal forest, dominated by black spruce trees, within the BOREAS northern study area in central Manitoba, Canada.	01/2002- 12/2003	Goulden et al. (2006)
Brookings	96.84W/ 44.35N	510	Grassland	Located in a private pasture, belonging to the Northern Great Plains Rangelands, the grassland is representative of many in the north central United States, with seasonal winter conditions and a wet growing season.	01/2005- 12/2006	Gilmanov et al. (2005)
Atqasuk	157.41W / 70.47N	15	Wet tundra	100 km south of Barrow, Alaska. Variety of moist-wet coastal sedge tundra, and moist-tussock tundra surfaces in the more well-drained upland.	01/2003- 12/2004	Oechel et al. (2014);
Ivotuk	155.75W / 68.49N	568	Alpine tundra	300 km south of Barrow and is located at the foothill of the Brooks Range and is classified as tussock sedge, dwarf-shrub, moss tundra.	01/2005- 12/2005	McEwing et al. (2015)

Table 4. Site description and measured volumetric soil moisture data used to validate TEM_Moss

Site	Location (Longitude (degrees) /Latitude (degrees))	Elevation (m)	Vegetation type	Data range	Citations
US-Ivo	155.75W/ 68.49N	579	Alpine tundra	01/2015-12/2016	Oechel & Kalhori (2018)
BOREAS NSA-OBS	98.48W/ 55.88N	259	Boreal forest	07/1995-06/1997	Stangel & Kelly (1999)
NL-Loo	5.74E/ 52.17N	25	Temperate coniferous forest	05/1997-12/1998	Falge et al. (2005)
DK-Sor	11.64E/ 55.49N	40	Temperate deciduous forest	01/1997-12/1999	Falge et al. (2005)
US-Bkg	96.84W/ 44.35N	510	Grasslands	01/2005-12/2006	Gilmanov et al. (2005)
US-Atq	157.41W/ 70.47N	25	Wet tundra	01/2015-12/2016	Oechel & Kalhori (2018)

Table 5. Site description and measured soil temperature at 5cm depth data used to validate TEM_Moss

Site	Location (Longitude (degrees) /Latitude (degrees))	Elevation (m)	Vegetation type	Data range	Citations
US-Ivo	155.75W/ 68.49N	579	Alpine tundra	01/2015- 12/2016	Oechel & Kalhori (2018)
BOREAS NSA-OBS	98.48W/ 55.88N	259	Boreal forest	01/1995- 12/1998	Stangel & Kelly (1999)
US-Ho1	68.74W/ 45.2N	60	Temperate coniferous forest	01/1996- 12/1997	Falge et al. (2005)
BE-Vie	6.0E/ 50.3N	493	Temperate deciduous forest	01/1997- 12/1998	Falge et al. (2005)
US-Bkg	96.84W/ 44.35N	510	Grasslands	01/2005- 12/2006	Gilmanov et al. (2005)
US-Atq	157.41W/ 70.47N	25	Wet tundra	01/2015- 12/2016	Oechel & Kalhori (2018)

Table 6. Model validation statistics for TEM_Moss and TEM 5.0 at six sites with NEP data

Site Name	Vegetation type	Models	Intercept	Slope	R-square	Adjusted R-square	RMSE	p-value
Ivotuk	Alpine tundra	TEM_Moss	0.46	0.61	0.72	0.70	3.57	<0.001
		TEM 5.0	-0.22	0.75	0.43	0.41	5.88	0.02
UCI-1964 burn site	Boreal forest	TEM_Moss	-0.13	1.01	0.91	0.90	8.33	<0.001
		TEM 5.0	-2.45	1.29	0.75	0.74	20.1	<0.001
Howland Forest (main tower)	Temperate coniferous forest	TEM_Moss	-1.28	1.05	0.83	0.81	19.69	<0.001
		TEM 5.0	-2.22	0.97	0.62	0.61	31.23	0.002
Bartlett Experimental Forest	Temperate deciduous forest	TEM_Moss	-0.49	1.03	0.94	0.94	19.06	<0.001
		TEM 5.0	-2.49	1.04	0.91	0.89	23	<0.001
Brookings	Grassland	TEM_Moss	0.36	1.02	0.85	0.84	8.95	<0.001
		TEM 5.0	2.58	0.75	0.62	0.6	13.07	<0.001
Atqasuk	Wet tundra	TEM_Moss	-0.36	0.97	0.84	0.83	5.13	<0.001
		TEM 5.0	1.99	0.75	0.75	0.74	6.56	<0.001

Table 7. Model validation statistics for TEM_Moss and TEM 5.0 at six sites with volumetric soil moisture data

Site ID	Vegetation type	Models	Intercept	Slope	R-square	Adjusted R-square	RMSE	p-value
US-Ivo	Alpine tundra	TEM_Moss	8.56	0.34	0.74	0.72	20.8	<0.001
		TEM 5.0	10.67	0.29	0.64	0.62	21.76	<0.001
BOREAS NSA-OBS	Boreal forest	TEM_Moss	10.71	0.51	0.52	0.51	11.1	<0.001
		TEM 5.0	16.47	0.43	0.32	0.31	11.96	<0.001
NL-Loo	Temperate coniferous forest	TEM_Moss	0.47	0.82	0.83	0.81	4.0	<0.001
		TEM 5.0	3.75	0.72	0.49	0.48	4.5	<0.001
DK-Sor	Temperate deciduous forest	TEM_Moss	1.39	0.86	0.67	0.65	3.65	<0.001
		TEM 5.0	10.41	0.54	0.4	0.39	4.06	<0.001
US-Bkg	Grassland	TEM_Moss	5.64	0.8	0.51	0.49	6.05	<0.001
		TEM 5.0	22.24	0.41	0.21	0.2	7.34	0.027
US-Atq	Wet tundra	TEM_Moss	7.76	0.77	0.87	0.85	7.38	<0.001
		TEM 5.0	6.74	0.68	0.85	0.84	7.63	<0.001

Table 8. Model validation statistics for TEM_Moss and TEM 5.0 at six sites with soil temperature at 5cm depth data

Site ID	Vegetation type	Models	Intercept	Slope	R-square	Adjusted R-square	RMSE	p-value
US-Ivo	Alpine tundra	TEM_Moss	-0.34	1.16	0.83	0.82	2.54	<0.001
		TEM 5.0	0.54	1.36	0.75	0.73	3.94	<0.001
BOREAS NSA-OBS	Boreal forest	TEM_Moss	-0.05	0.91	0.9	0.88	2.24	<0.001
		TEM 5.0	0.27	0.81	0.84	0.82	2.9	<0.001
US-Ho1	Temperate coniferous forest	TEM_Moss	0.7	0.95	0.81	0.79	2.93	<0.001
		TEM 5.0	-0.06	0.99	0.77	0.76	3.41	<0.001
BE-Vie	Temperate deciduous forest	TEM_Moss	0.57	0.92	0.83	0.81	1.82	<0.001
		TEM 5.0	1.88	0.85	0.69	0.68	2.56	<0.001
US-Bkg	Grassland	TEM_Moss	0.17	0.87	0.91	0.89	2.87	<0.001
		TEM 5.0	-0.01	0.91	0.89	0.87	3.04	<0.001
US-Atq	Wet tundra	TEM_Moss	1.36	0.86	0.84	0.82	3.63	<0.001
		TEM 5.0	4.33	0.99	0.75	0.74	6.17	<0.001

Table 9. Average annual NPP, R_H and NEP (as Pg C per year) during the 20th century estimated by two models.

Average annual carbon fluxes (Pg C yr^{-1})		TEM_Moss	TEM 5.0	Difference	Moss NPP/ Vascular plants NPP
NPP	Moss NPP	1.69	-	-	21.3%
	Vascular plants NPP	7.93	8.8	-	
	Total NPP	9.6	8.8	0.8	
R_H		7.38	7.91	-0.53	
NEP		2.22	0.89	1.33	

Table 10. Increasing of SOC, vegetation carbon (VGC), and moss carbon (MOSSC) from 1900 to 2000, and total carbon storage during the 20th century predicted by two models.

Models	Carbon pools	Carbon pool amounts in 1900/2000 (units: Pg)	Changes in carbon pools during the 20th century (units: Pg)
TEM_Moss	SOC	587.1/683.4	96.3
	VEGC	297.5/412.7	115.2
	MOSSC	19.6/30	10.4
	Total	904.2/1126.1	221.9
TEM 5.0	SOC	583.2/614.9	31.7
	VEGC	291.1/348.6	57.5
	Total	874.3/963.5	89.2

Table 11. Average annual NPP, R_H and NEP (as Pg C per year) during the 21st century estimated by two models under (a) RCP 8.5 scenario and (b) RCP 2.6 scenario.

(a)

Average annual carbon fluxes (Pg C yr⁻¹)		TEM_Moss	TEM 5.0	Difference	Moss NPP/ Vascular plants NPP
NPP	Moss NPP	3.84	-	-	38.4%
	Vascular plants NPP	10	12.53	-	
	Total NPP	13.84	12.53	1.31	
R_H		11.28	11.54	-0.21	
NEP		2.56	0.99	1.57	

(b)

Average annual carbon fluxes (Pg C yr⁻¹)		TEM_Moss	TEM 5.0	Difference	Moss NPP/ Vascular plants NPP
NPP	Moss NPP	3.74	-	-	40.5%
	Vascular plants NPP	9.24	11.52	-	
	Total NPP	12.98	11.52	1.46	
R_H		10.91	11.24	-0.33	
NEP		2.07	0.28	1.79	

Table 12. Increasing of SOC, vegetation carbon (VGC), and moss carbon (MOSSC) from 1900 to 2000, and total carbon storage during the 21st century predicted by two models under (a) RCP 2.6 scenario and (b) RCP 8.5 scenario.

(a)

Models	Carbon pools	Carbon pool amounts in 2000/2099 (units: Pg)	Changes in carbon pools during the 21st century (units: Pg)
TEM_Moss	SOC	608.1/692.8	84.7
	VEGC	320.2/432.8	112.6
	MOSSC	26.2/35.6	9.4
	Total	954.5/1161.2	206.7
TEM 5.0	SOC	604.4/616.5	12.1
	VEGC	318.2/333.7	15.5
	Total	922.6/950.2	27.6

(b)

Models	Carbon pools	Carbon pool amounts in 2000/2099 (units: Pg)	Changes in carbon pools during the 21st century (units: Pg)
TEM_Moss	SOC	615.9/708.4	92.5
	VEGC	327.8/481.4	153.6
	MOSSC	28.1/38.2	10.1
	Total	971.8/1228.0	256.2
TEM 5.0	SOC	610.2/654.4	44.2
	VEGC	324.9/379.4	54.5
	Total	935.1/1033.8	98.7